

Physical Origin of Selectivity in Ionic Channels of Biological Membranes

Alessandro Laio^{*#} and Vincent Torre^{*#}

^{*}Istituto Nazionale per la Fisica della Materia, Unita' di Trieste, and [#]Scuola Internazionale di Studi Superiori Avanzati, Trieste, Italy

ABSTRACT This paper shows that the selectivity properties of monovalent cation channels found in biological membranes can originate simply from geometrical properties of the inner core of the channel without any critical contribution from electrostatic interactions between the permeating ions and charged or polar groups. By using well-known techniques of statistical mechanics, such as the Langevin equations and Kramer theory of reaction rates, a theoretical equation is provided relating the permeability ratio P_B/P_A between ions A and B to simple physical properties, such as channel geometry, thermodynamics of ion hydration, and electrostatic interactions between the ion and charged (or polar) groups. Diffusive corrections and recrossing rates are also considered and evaluated. It is shown that the selectivity found in usual K^+ , gramicidin, Na^+ , cyclic nucleotide gated, and end plate channels can be explained also *in the absence of any charged or polar group*. If these groups are present, they significantly change the permeability ratio only if the ion at the selectivity filter is in van der Waals contact with them, otherwise these groups simply affect the channel conductance, lowering the free energy barrier of the same amount for the two ions, thus explaining why single channel conductance, as it is experimentally observed, can be very different in channels sharing the same selectivity sequence. The proposed theory also provides an estimate of channel minimum radius for K^+ , gramicidin, Na^+ , and cyclic nucleotide gated channels.

INTRODUCTION

The production and propagation of nerve impulses along neuronal structures and across synapses rely on the existence of ionic channels specific to Na^+ and K^+ : these highly selective channels provide the basis for electrical signaling in the nervous system and ultimately for information processing in the brain. The understanding of physical mechanisms underlying the ionic selectivity of these channels is a key issue in contemporary biophysics and cell physiology (Hille, 1992).

In 1962 Eisenman provided a very simple and elegant theory of ionic selectivity, inspired by the selectivity of special glasses to bind specific ions (see also Eisenman, 1963; Krasne and Eisenman, 1973; Eisenman and Krasne, 1975). Selectivity was explained as originating from the difference between the hydration free energy of the ion and the energy of the interaction between the ion and a charged binding site within the channel. This theory correctly predicted the existence of XI selectivity sequences, usually found in biological ionic channels. The notion that ionic selectivity is primarily produced by electrostatic interactions of the ion with charged and/or polar groups within the channel has been subsequently developed by several authors (Eisenman and Horn, 1983; Reuter and Stevens, 1980) and represents the core of the present understanding of ionic selectivity.

The possibility of mutating amino acids at given locations of an ionic channel by using genetics and molecular biology has provided significant information on the role of specific

amino acids. For instance, it is now well established that charged and polar residues control single channel conductance in ionic channels (Imoto et al., 1988), the selectivity between monovalent and divalent cations (Heinemann et al., 1992; Kim et al., 1993; Yang et al., 1993) and the selectivity between cations and anions (Galzi et al., 1992; Roux, 1996; Dorman et al., 1996). In these experiments a Na^+ channel was mutated in a Ca^{2+} channel by single point mutation and a cationic channel was mutated in an anionic channel by changing a restricted number of amino acids. K^+ and Na^+ channels have extensively mutated (Faure et al., 1996; Fuller et al., 1997; Chiamvimonvat et al., 1996; Heginbotham et al., 1994; Yool and Schwartz, 1991; Slesinger et al., 1993; Kirsch et al., 1995) but so far it has not been possible to mutate a K^+ channel in a Na^+ channel (and vice versa) by changing charged and/or polar residues. As a consequence, it has not been possible to identify a restricted number of charged and/or polar groups responsible for the selectivity between Na^+ and K^+ , and the notion that electrostatic interactions within the channel determine the selectivity between Na^+ and K^+ of an ionic channel is not supported by the extensive experimentation carried out so far.

The purpose of this paper is to analyze whether the selectivity among monovalent cations, such as Na^+ and K^+ , of ionic channels may originate from simple physical mechanisms, different from the electrostatic interactions so far proposed. Two observations are at the basis of the proposed theory. First, Na^+ and K^+ channels in different tissues and animals have a different amino acid sequence but a common structural feature: K^+ channels are permeable only to small cations and their narrowest radius is ~ 1.5 Å. On the contrary, Na^+ channels are also permeable to a variety of organic cations and their narrowest restriction has been estimated to be $\sim 3.1 \times 5.1$ Å (see Hille, 1992). Second, the common feature of ionic permeation in all K^+ (or Na^+) channels with a different amino acid sequence is the ther-

Received for publication 2 February 1998 and in final form 10 September 1998.

Address reprint requests to Dr. Vincent Torre, Scuola Internazionale di Studi Superiori Avanzati, Via Beirut 2, 34014 Trieste, Italy. Tel.: 39-40-2240-470; Fax: 39-40-2240-470; E-mail: torre@sissa.it.

© 1999 by the Biophysical Society

0006-3495/99/01/129/20 \$2.00

modynamics of K^+ (or Na^+) hydration, that is, the physical mechanisms by which water molecules interact with permeating ions.

This paper provides a theoretical relation linking the permeability ratio P_A/P_B to simple physical properties of the channel, such as its radius and other molecular properties. This theoretical relation allows us to evaluate the physical mechanisms underlying ionic selectivity: by taking into account the thermodynamics of ion hydration, it is possible to numerically compute the permeability ratio P_A/P_B between alkali monovalent cations and compare the contribution of geometrical factors and electrostatic interactions. The present paper shows that selectivity of ionic channels among monovalent alkali cations can be explained from a semiquantitative point of view, simply in terms of the size of the inner core of the channel and of the thermodynamics of ion hydration, without any significant contribution from electrostatic interactions with charged or polar groups within the pore.

This paper is organized in five sections. The first reviews previous approaches used to describe ionic permeation and selectivity. The aim of the second section is to provide a theoretical equation (Eq. 6) linking the permeability ratio P_A/P_B between ions A and B and some physical quantities describing the channel. This equation is obtained from Langevin equations in the case of strong friction and from Kramer rate theory (KRT) in the case of moderate-to-strong friction. The third section presents an explicit model of the selectivity filter, and the permeability ratio P_A/P_B is computed for monovalent alkali cations. The fourth section reviews experimental results on ionic selectivity among monovalent cations for K^+ , gramicidin, Na^+ , cyclic nucleotide gated (CNG), and end plate channels in the light of the proposed approach for understanding ionic selectivity. The fifth section is a discussion of the results.

PREVIOUS APPROACHES

Our understanding of ionic selectivity in membrane channels relies primarily on the pioneering work of Eisenman (Eisenman, 1962; Eisenman and Krasne, 1975; Eisenman and Horn, 1983) on glass electrodes and selective chelators. Briefly, an ion with charge q and radius r has a hydration free energy represented by the Born approximation:

$$G_{\text{hydr}} = \frac{q^2}{8\pi\epsilon_w r} \quad (1)$$

where ϵ_w is the dielectric constant of water and its electrostatic interaction with a site within the channel of charge q_s and radius r_s is:

$$G_{\text{int}} = \frac{qq_s}{4\pi\epsilon_w(r + r_s)} \quad (2)$$

Ionic selectivity depends on the difference between G_{hydr} and G_{int} : indeed by changing the radius r_s of the charged site it is possible to obtain 11 selectivity sequences, which are usually found in biological channels (Eisenman, 1962,

1963). The Born approximation is physically sound, although it assumes that the solvent is a continuum dielectric medium. Furthermore, because the model is based on a very small number of parameters, it was possible to explore a large range of plausible situations and show the consequences. The strong point of the Eisenman theory is that only very specific selectivity sequences came out of this analysis. Recently, the role of electrostatic interactions in ionic selectivity has been reinterpreted as being a result of interactions between the permeating cation and π electrons of aromatic residues (Kumpf and Dougherty, 1993).

A more detailed analysis of ionic permeation through biological channels can be obtained by two different approaches: molecular dynamics simulations and Kramer rate theory (see Appendix A). Molecular dynamics has been used to understand several properties of ionic permeation in gramicidin (or gramicidin-like) channels using either classical dynamics (Roux and Karplus, 1991, 1993, 1994; Roux, 1996; Dorman et al., 1996) or ab initio methods (Segonella et al., 1996). These approaches have provided important information on the location and properties of wells and barriers and on the role of amino acid side chain motion. Several authors (Eyring et al., 1949; Woodbury, 1971; Lauger, 1973; Hille, 1975a) have proposed a description of the permeation of an ion through a membrane channel as the motion of the ion through a potential energy profile (see Fig. 1 A). This energy profile is usually composed by wells, corresponding to binding sites and by barriers, corresponding to activated states. These approaches were largely based on KRT and in several occasions provided an excellent description of the experimental data (Hille, 1975b; Perez-Cornejo and Begenish, 1994). However, these approaches assumed the validity of Transition State Theory (TST) and rate constants were as in Eq. A.5, thus neglecting friction and assuming a transmission factor equal to 1. However, when an ion moves in a liquid and/or in a channel, it continuously interacts with the water molecules and atoms forming the channel so that friction cannot be neglected (Cooper et al., 1985, 1988a, b; Andersen, 1989). In addition, it is not possible to neglect diffusion phenomena, which are likely to be relevant during the permeation process. As a consequence, the use of rate constants as in Eq. A.5 with χ equal to 1, as in the TST approach, to describe ionic permeation through biological channels is not justified, and it is necessary to use either Langevin equations or rate constants with appropriate corrections, as discussed in Appendix A.

The present paper uses Langevin and Fokker-Planck equations similarly to Levitt (1991) and Bek and Jacobsson (1994) and some of their equations are very similar to the ones derived here (for instance, Eq. 8). Also, the analysis of selectivity of Wu (1991) has some similarity with the one proposed here: in both cases the selectivity sequence predicted when the channel radius is 1.6 and 2.2 Å is the same.

THE PERMEABILITY RATIO

This section is the theoretical core of the paper. A quantitative description of ionic permeation can be greatly sim-

plified by assuming that the dynamics of the problem is essentially classic and that quantum mechanical effects are taken into account by appropriate potential functions in the full phase space A of the permeating ion, the channel, the water, and lipid environment. To reduce the complexity of the problem, a common practice in physics is to evaluate the possibility of reducing the dimensions of the phase space A . This reduction of complexity can be obtained when the underlying dynamics occurs on different time scales so that some variables are slow and others fast. In dynamical system theory (Arnold, 1985) fast variables of a dynamical system can be neglected by appropriate averaging techniques and the original dynamical system is approximated with a reduced dynamical system, where fast variables have been eliminated. A similar approach has been introduced also in statistical mechanics, leading to Langevin equations and KRT (Gardiner, 1985; Risken, 1989; Melnikov, 1991; Hanggi et al., 1990). In this case the action of fast variables is described by a random force, leading to a stochastic differential equation, i.e., a Langevin equation. In order to describe the evolution of a complex system (such as ions permeating through a biological channel), it is useful to introduce a *reaction coordinate* $x(t)$, corresponding to some physical observable quantity (in our case the reaction coordinate is the position of the permeating ion). The dynamics of the pair $X(t) = (x(t), x'(t))$ is the result of a reduced description from the full space $A \rightarrow X(t)$. This reduction of complexity is obtained by introducing new quantities, i.e., entropy and friction. The entropy factor concerns the reduction of all coupled degrees of freedom from a high dimensional potential energy in A to the effective potential for the reduced dynamics of $X(t)$. This effective potential is usually referred to as the mean field potential and is composed of a series of barriers and wells (see, e.g., Fig. 1 A). Similarly, friction concerns the reduced action of the degrees of freedom that are lost during the contraction from A to $X(t)$.

The major theoretical result of this section is the derivation of a general equation relating the permeability ratio P_B/P_A among monovalent cations A and B to physical properties of the channel (see Eq. 6). The permeability ratio is defined, as usual, from the reversal potential under biionic conditions.

Let us consider a membrane of thickness l with two monovalent cations A and B present at the opposite sides, so that $[A]_o = \rho_A$, $[B]_i = \rho_B$ and $[A]_i = [B]_o = 0$ where $[I]$ denotes the concentration of ion I . The *permeability ratio* of A with respect to B (when $\rho_A = \rho_B$) is defined as:

$$\frac{P_B}{P_A} = \exp(\beta F V_{\text{rev}}) \quad (3)$$

where F is the Faraday constant and V_{rev} is the potential that has to be applied to the channel in order to have $j_A + j_B = 0$, where $j_A(j_B)$ is the flow of ion A(B). Denoting by $G_I(x)$ the Gibbs free energy profile along for ion I , the location x_A and x_B of the two ions A and B in the channel can be

obtained from the coupled Langevin equations:

$$M_A \ddot{x}_A + \frac{dG_A}{dx_A} + \gamma_A \dot{x}_A + \frac{dv(x_A, x_B)}{dx_A} = \xi_A(t) \quad (4)$$

$$M_B \ddot{x}_B + \frac{dG_B}{dx_B} + \gamma_B \dot{x}_B + \frac{dv(x_A, x_B)}{dx_B} = \xi_B(t) \quad (5)$$

where M is the ion mass, γ is the friction, $\xi(t)$ is a white noise (see Appendix A or Melnikov, 1991) and $v(x_A, x_B)$ is an (effective) interaction potential between the two ions. It is well known that the ionic selectivity depends rather weakly on ionic activity, thus suggesting that ionic selectivity does not originate from ion-ion interactions within a channel (see chapter 13 of Hille, 1992, and references included). Indeed, when the concentration ρ is low so that at most only one ion is present in the channel, the interaction between the two ions A and B can be neglected, i.e., $dv(x_A, x_B)/dx_A \sim 0$ and $dv(x_A, x_B)/dx_B \sim 0$. In this case, the motion of the two ions occurs almost independently, but ionic selectivity is present, almost unaffected. The effect of ion-ion interaction on the total flux and on ionic selectivity will be discussed elsewhere (Laio and Torre, in preparation). In what follows, we will show that the permeability ratio between two ions A and B has the simple form

$$\frac{P_B}{P_A} = \frac{\tau_B}{\tau_A} \exp(-\beta(G_B^{(s)} - G_A^{(s)})) \quad (6)$$

where $\beta = 1/RT$ (R is the gas constant and T the absolute temperature), $G_{A(B)}^{(s)}$ is the Gibbs free energy of ion A(B) at the highest barrier that, in the following, will be called *selectivity filter* and denoted by s , and $\tau = \tau(\gamma, M, G''(x_s), \dots)$ is a prefactor, depending on friction, ionic mass, and free energy profile.

In the next section friction is assumed to be very high, so that the inertia term ($M\ddot{x}$) in the Langevin equation can be neglected. In this case (i.e., the strong friction case) an explicit equation for the permeability ratio is obtained (i.e., Eq. 12). The following section treats the moderate-to-strong friction case in which rates of reaction are described in the KRT approximation and also in this case an explicit equation (i.e., Eq. 18) for the permeability is obtained. The subsequent summary shows that, in a large variety of cases, τ_B/τ_A is close to 1, so that P_B/P_A is primarily determined by the exponential factor.

Strong friction case: Langevin equations

Let us now consider the case in which the friction factor is so large that the inertial terms $M_A \ddot{x}_A$ and $M_B \ddot{x}_B$ can be neglected. This is the strong friction case already considered by previous authors (Andersen, 1989). In this case the solution of the Langevin equation can be obtained by solving the associated Fokker-Planck equation as shown in Appendix B. After some algebra (see Appendix B) the

following equation for the permeability ratio is obtained:

$$\frac{P_B}{P_A} = \frac{D_B}{D_A} \exp(-\beta(G_B^{(s)} - G_A^{(s)})) \quad (7)$$

$$\frac{\int_0^l dx \exp[-\beta \Delta G_A(x)] (P_B/P_A)^{-x/l}}{\int_0^l dx \exp[-\beta \Delta G_B(x)] (P_B/P_A)^{-x/l}}$$

where $D_{(A,B)} = RT/M_{(A,B)}\gamma_{(A,B)}$ is the diffusion coefficient and $\Delta G_{(A,B)}$ is defined by:

$$G_{(A,B)}^{(s)} - \Delta G_{(A,B)}(x) = G_{(A,B)}(x) \quad (8)$$

By definition, $\Delta G_{(A,B)}(x)$ is always positive and rather large at wells. As a consequence the integrals in Eq. 7 are primarily determined by the free energy profile near the barriers. For instance, the contribution to the selectivity ratio of a well x_w such that $\beta \Delta G(x_w) = 4$, compared to the contribution of the highest barrier, is in the order of 1%. This example indicates that wells, i.e., binding sites, are not crucial for ionic selectivity and that, in the range of validity of Langevin equation, the permeability ratio is almost independent of the depth of the wells (see also Hille, 1975a, b). Notice also that, when $\Delta G_A(x) \sim \Delta G_B(x)$, Eq. 8 can be significantly simplified, as the two integrals cancel each

other and becomes:

$$\frac{P_B}{P_A} = \frac{D_B}{D_A} \frac{Z_B}{Z_A} \quad (9)$$

where $Z_B(Z_A)$ is the partition function of ions $A(B)$ in s . The condition $\Delta G_A(x) \sim \Delta G_B(x)$ is equivalent to the well-known offset peak condition (see Hille, 1992).

Moderate-to-strong friction: Kramer rate theory

Often, the strong friction assumption is not a good approximation. For instance, when the free energy profile $G(x)$ varies significantly on the scale of the mean free path of the ion within the channel, it is not possible to neglect inertial effects, as assumed in the previous section. Therefore, in this section we will consider the moderate-to-strong friction case where reaction rates provided by KRT will be used (see Appendix A).

Let us assume that the permeation through the ionic channel is described as the crossing through M barriers separated by $M - 1$ wells (see Fig. 1 A). We will assume biionic conditions in which ion A is on the left side of the membrane channel, with concentration $[A]_L$, and ion B on the right, with concentration $[B]_R$. As shown in Appendix B,

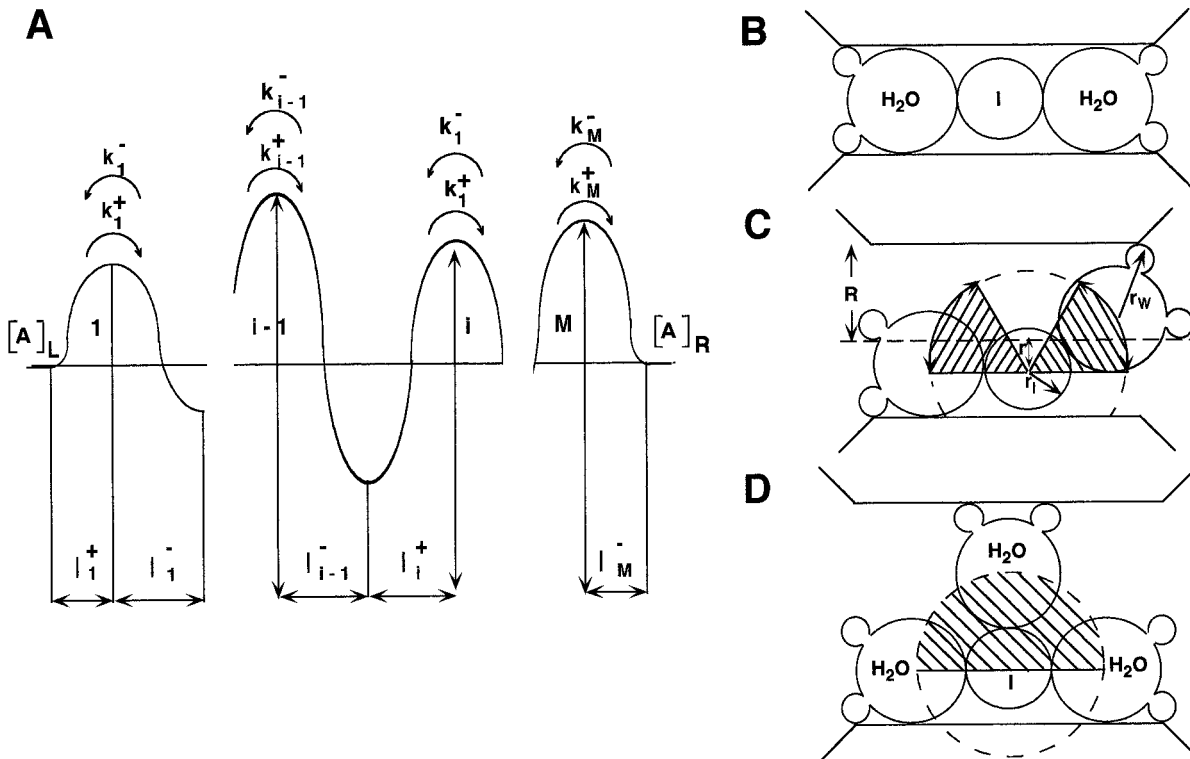


FIGURE 1 (A) The Gibbs energy profile $G(x)$ composed by M barriers and $M - 1$ wells. k_{i-1}^+ is the rate constant across barrier $i - 1$ from left to right and k_{i-1}^- from right to left. l is the usual electrical distances. (B–D) The local geometry of the channel at the selectivity filter. R is the local channel radius, r_i is the ion radius, r_w is the radius of a water molecule, and r is the distance from the channel axis of the ion in cylindrical coordinates. (B) $R = r_w$; (C) $r_w < R < r_i + r_w$; (D) $r_i + r_w < R < 2(r_i + r_w)$. The shaded area is an indication of the extent of the solid angle Ω accessible to water; in (B) Ω is equal to 0, while in (D) it is 2π .

using Eq. 3, we obtain that the permeability ratio is the solution of the nonlinear equation:

$$\frac{P_B}{P_A} = \frac{\sum_{i=1}^M \exp[\beta \mathcal{G}_{A,i}] \left(\frac{P_B}{P_A} \right) \exp\left(\sum_{h=i+1}^M l_h^+ - \sum_{h=1}^{i-1} l_h^- \right)}{\sum_{i=1}^M \exp[\beta \mathcal{G}_{B,i}] \left(\frac{P_B}{P_A} \right) \exp\left(\sum_{h=i+1}^M l_h^+ - \sum_{h=1}^{i-1} l_h^- \right)} \sqrt{\frac{M_A}{M_B}} \quad (10)$$

where

$$\mathcal{G}_{l,i} = G_{l,i} + \frac{1}{\beta} \ln \left(\sqrt{\frac{\zeta_{l,i}^2}{4} + 1} - \frac{\zeta_{l,i}}{2} \right)$$

with

$$\zeta_{l,i} = \gamma_l \left(\frac{1}{M_l} G_l''(x_{s,i}) \right)^{-1/2}$$

(see Appendix A) and l_i^+ (l_i^-) is the electric distance between well $i-1$ and the barrier i (between well i and barrier i); the logarithmic term takes into account diffusive corrections (see Appendix A).

Similarly to the strong friction case, also in the moderate-to-strong friction regime, $G^{(w)}$ values simplify exactly, i.e., within a KRT approximation, P_B/P_A is *independent* of the free energy at the wells (see also Hille, 1975a, b).

By using Eq. 10 it is possible to discuss the effect of “secondary” barriers on P_B/P_A , assuming them to be some RT lower than the highest one (if this is not true, one should solve Eq. 10 in its full generality). Denoting by s the highest barrier, and defining

$$\mathcal{G}_{(A,B),s} - \mathcal{G}_{(A,B),i} = \Delta \mathcal{G}_{(A,B),i} \geq 0 \quad (11)$$

the solution of Eq. 10 up to linear order in $\exp(-\beta(\min_{i \neq s} \{\Delta \mathcal{G}_{A,i}, \Delta \mathcal{G}_{B,i}\}))$ has the form:

$$\frac{P_B}{P_A} = \rho_0 (1 + \pi)$$

where ρ_0 is the single-barrier permeability ratio

$$\rho_0 = \sqrt{\frac{M_A}{M_B}} \frac{\sqrt{\frac{\zeta_B^2}{4} + 1} - \frac{\zeta_B}{2}}{\sqrt{\frac{\zeta_A^2}{4} + 1} - \frac{\zeta_A}{2}} \exp[-\beta(G_{B,s} - G_{A,s})] \quad (12)$$

and, denoting by $\lambda_{i,s}$ the electric distance between barrier i and barrier s ,

$$\begin{aligned} \pi = & \sum_{i < s} (\exp[-\beta \Delta \mathcal{G}_{A,i}] - \exp[-\beta \Delta \mathcal{G}_{B,i}]) (\rho_0)^{\lambda_{i,s}} \\ & + \sum_{i > s} (\exp[-\beta \Delta \mathcal{G}_{A,i}] - \exp[-\beta \Delta \mathcal{G}_{B,i}]) (\rho_0)^{-\lambda_{i,s}}. \end{aligned}$$

π gives the corrections to the single-barrier permeability ratio ρ_0 because of the presence of secondary barriers. This correction is small if $\Delta \mathcal{G}_{A,i} \sim \Delta \mathcal{G}_{B,i}$ (i.e., in the offset peak condition), but also if $\exp[-\beta \Delta \mathcal{G}_{A,i}]$ and $\exp[-\beta \Delta \mathcal{G}_{B,i}]$ are small with respect to 1 for all i . In this case, we do not need to keep explicitly into account all the barrier of the free energy profile along the channel, since P_B/P_A is basically determined by the highest barrier alone, and within the range of validity of a KRT approach P_B/P_A has the simple form of Eq. 6, with

$$\frac{\tau_B}{\tau_A} = \sqrt{\frac{M_A}{M_B}} \frac{\sqrt{\frac{\zeta_B^2}{4} + 1} - \frac{\zeta_B}{2}}{\sqrt{\frac{\zeta_A^2}{4} + 1} - \frac{\zeta_A}{2}} \quad (13)$$

Evaluation of τ_B/τ_A

Let us review the expression obtained for τ_B/τ_A in the different cases and discuss its dependence on the various parameters involved in our model, i.e., the diffusion constant, ionic mass, and barrier height. It will be shown that the ratio $(\tau_B/\tau_A)/(D_B/D_A)$ does not depend on the ion mass in the strong friction case and when barriers are low, but it depends on the ion mass in the KRT case. The major conclusion of this section, illustrated in Fig. 2, is that the ratio $(\tau_B/\tau_A)/(D_B/D_A)$ varies at most by less than an order of magnitude in a large range of cases, indicating that the predominant factor in the determination of the permeability ratio (Eq. 6) is the exponential factor.

In the moderate-to-strong friction case (i.e., in the KRT approximation), τ_B/τ_A has the form:

$$\left(\frac{\tau_B}{\tau_A} \right)_{\text{krt}} = \sqrt{\frac{M_A}{M_B}} \frac{\sqrt{\zeta_B^2/4 + 1} - \zeta_B/2}{\sqrt{\zeta_A^2/4 + 1} - \zeta_A/2} \quad (14)$$

(the subscript krt stands for Kramer rate theory).

When both ζ_A and ζ_B are large with respect to 1 (i.e., in the strong friction case), we have

$$\frac{\tau_B}{\tau_A} \rightarrow \left(\frac{\tau_B}{\tau_A} \right)_{\text{sf}} = \sqrt{\frac{M_A}{M_B}} \frac{\zeta_A}{\zeta_B} = \frac{D_B}{D_A} \sqrt{\frac{G_B''(x_s)}{G_A''(x_s)}}. \quad (15)$$

(the subscript sf stands for *strong friction*). If ζ_A and ζ_B are almost 0 (this happens if $G''(x_s)$ is large, i.e., if the barrier is narrow and high) $(\tau_B/\tau_A)_{\text{krt}}$ approaches the TST limit $\sqrt{M_A/M_B}$.

If also the highest barrier in the channel is lower than some RT , one should in principle use Eq. 8 in its full generality, i.e., it is necessary to explicitly integrate the entire free energy profile. In these conditions, the permeability ratios are small and highly dependent on the specific structure of the channel.

Let us suppose that the free energy profile has the form

$$G(x) = \begin{cases} \left(1 - \left(\frac{2x}{\lambda}\right)^2\right) & x \in \left[-\frac{\lambda}{2}, \frac{\lambda}{2}\right] \\ 0 & \text{otherwise} \end{cases} \quad (16)$$

where λ is the barrier width and that friction is so high that Eq. 8 can be used. Neglecting the $(P_B/P_A)^{x/1}$ factors in calculating the integrals in Eq. 8 we obtain:

$$\frac{P_B}{P_A} \approx \frac{D_B}{D_A} \frac{\sqrt{G_B/RT} \operatorname{erf}(\sqrt{G_A/RT})}{\sqrt{G_A/RT} \operatorname{erf}(\sqrt{G_B/RT})} \exp(-\beta(G_B^{(s)} - G_A^{(s)})) \quad (17)$$

and in the case of low barriers we obtain:

$$\frac{\tau_B}{\tau_A} = \left(\frac{\tau_B}{\tau_A}\right)_{\text{lb}} = \frac{D_B}{D_A} \frac{\sqrt{G_B/RT} \operatorname{erf}(\sqrt{G_A/RT})}{\sqrt{G_A/RT} \operatorname{erf}(\sqrt{G_B/RT})} \quad (18)$$

(the subscript lb stands for *low barriers*).

This formula provides the correct limit for G_B and G_A equal to zero, i.e.,

$$\frac{P_B}{P_A} = \frac{D_B}{D_A}. \quad (19)$$

Moreover, if the barriers are high enough, $\operatorname{erf}(\sqrt{G/RT}) \rightarrow 1$ and the permeability ratio reduces to that obtained in the strong friction case.

To evaluate the differences between the three expressions for τ_B/τ_A (i.e., Eqs. 14, 15, and 18) a numerical example is useful. It is evident from Eqs. 15 and 18 that the ratio $(\tau_B/\tau_A)/(D_B/D_A)$ does not depend on the ion, and depends on the ion mass only in the KRT case. As a consequence, in Fig. 2 the ratio $(\tau_A/\tau_{Li})/(D_A/D_{Li})$ is plotted against G_B/RT for K^+ , Na^+ , Rb^+ , and Cs^+ , in the three different cases, i.e., strong friction case (\square), KRT case (*continuous line*), and

low barrier case (\circ). The values $G_{Li}/RT = 10$ and $\lambda = 6 \text{ \AA}$ (λ is the thickness of the barrier as defined by Eq. 16) were chosen as reference. It is evident that all lines superimpose at some extent and no major differences are observed. However, some remarks are useful. In the strong friction case (\square) $D_{Li}\tau_B/D_B\tau_{Li}$ goes to zero for $G_B \rightarrow 0$, suggesting that if G_B is small, diffusive correction might become crucial. However, in these conditions, a rate theory cannot be reliably used (even if friction is very strong) and the full Langevin equation must be solved.

The behavior of $D_{Li}\tau_B/D_B\tau_{Li}$, as predicted by the Kramer theory, depends on the ion (in fact, with moderate friction, inertia becomes important). This is the correct behavior of τ_B/τ_{Li} in the high barrier regime. The difference from the strong friction prediction is always small, and completely negligible for $G_B/RT < \sim 15$. The KRT case approaches the value of $\sqrt{M_B/M_{Li}}$, i.e., the TST prediction, only for very high values of G_B/RT .

In the low barrier case (\circ) the correct behavior for $G_B \rightarrow 0$ is observed: $(\tau_B/\tau_{Li})/(D_B/D_{Li})$ goes to a non-zero constant for $G_B \rightarrow 0$, and to 1 if also $G_A \rightarrow 0$, i.e., τ_B/τ_{Li} goes to the diffusive limit D_B/D_{Li} .

Summary of results

The results described in this section were obtained by making the following assumptions: 1) The ionic permeation through a biological channel can be described as the motion along a single reaction coordinate x . This implies that the relevant dynamics on the other degrees of freedom occurs on different time scales. 2) Thermodynamic equilibrium prevails on the fast moving degrees of freedom, so that it is possible to consider a mean field potential, i.e., a Gibbs free energy $G(x)$ depending on the reaction coordinate x . 3) Electrostatic interactions between two permeating ions can be neglected.

The existence of discrete events observed in electrophysiological single channel recordings indicates that in a time scale of $10 \div 100 \mu s$ (the time scale of these recordings), thermodynamic equilibrium is probably reached in a significant portion of the full phase space. The third assumption, i.e., the possibility of neglecting interactions between permeating ions, is supported by the observation that ionic selectivity does not change significantly when ion-ion interactions are reduced or even removed by lowering the concentration of permeating ions. Under these assumptions the permeability ratio P_A/P_B (see Eq. 3) is described under biionic conditions by Eq. 6.

The form (Eq. 18) for τ_B/τ_A gives a good semiquantitative estimation of recrossing corrections to permeability ratio except if the barriers are very high (over $30 RT$) and will be used to compute permeability ratios in the next two sections. Notice also that the contribution of these corrections to the permeability ratio is *always small*, except for quite pathological situations (i.e., when G_B is very large and G_A close to 0, or vice versa). For instance, in the example discussed in Fig. 2, $(\tau_B/\tau_A)/(D_B/D_A)$ ranges from 0.5 (for $G_B = 0$) to 5 (for $G_B = 30 RT$), while in the same conditions

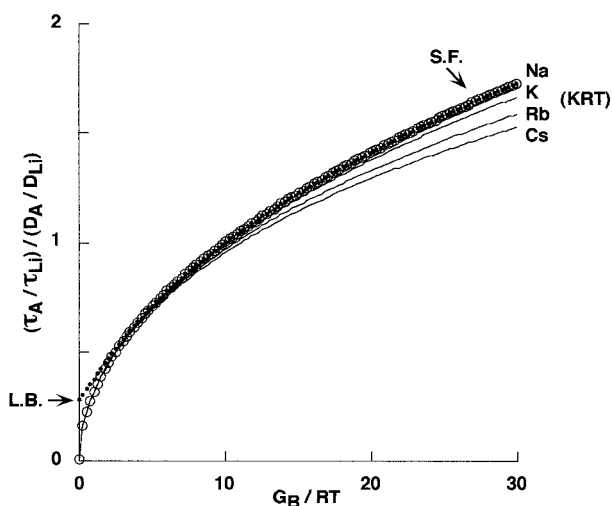


FIGURE 2 The relation between $(\tau_A/\tau_{Li})/(D_A/D_{Li})$ and the barrier height (G_B/RT) in different regimes. Dots were obtained from the full Langevin equation (i.e., Eq. 18), the circles were obtained in the strong friction case (i.e., Eq. 15), and the thin lines were obtained from the KRT approximation (i.e., Eq. 14) for Na^+ , K^+ , Rb^+ , and Cs^+ , as indicated by the arrows.

Z_B/Z_A is e^{10} and e^{-20} , respectively. Thus, far more important in determining the permeability ratio is the exponential factor $\exp(-\beta(G_B^{(s)} - G_A^{(s)})) = Z_A/Z_B$ (see also the contribution of τ_B/τ_A to permeability ratios section). This, and not the recrossing correction, determines the *order of magnitude* of P_B/P_A . This property, together with the weak dependence of P_B/P_A on the free energy profile at wells and at barriers, except the highest one is the main reason why structurally different channels have similar selectivity properties, as experimentally observed. The goal of next section is to provide a reliable model for calculating the free energy at the selectivity filter s .

COMPUTATION OF THE GIBBS FREE ENERGY

Equation 6, derived in the previous section, relates the permeability ratio P_A/P_B to the Gibbs free energy of ions A and B at the selectivity filter.

To compute the permeability ratio effectively, it is necessary to evaluate the free energy profile of the ion inside the channel. By definition we have:

$$Z(x) = \int_C \delta(x - c) e^{-\beta H} dc \quad (20)$$

$$G(x) = -\frac{1}{\beta} \ln Z(x)$$

where H is the Hamiltonian of the ion at the selectivity filter, C is the entire configuration space, and $\delta(x)$ is the Dirac function. It is important now to observe that the highest barrier of the Gibbs free energy profile $G(x)$ corresponds to a saddle point of the Hamiltonian H in the full phase space A . The exact location of this saddle point depends on the specific molecular structure of the system ion-water channel, but is expected to be at some distance from charged and polar groups. Indeed, the most unfavorable location for the ion inside the channel is the region *between* two charged and polar groups. Thus, by definition of saddle point, the permeating ion at the selectivity filter cannot be in contact with charged and polar groups, i.e., the permeating ion does not interact chemically with these charged and polar groups, and the electronic states of the permeating ion do not undergo significant rearrangements. A recent remarkable paper (Doyle et al., 1998) has identified the selectivity filter of a K^+ channel in crystallographic data, located between two binding sites separated by ~ 7.5 Å.

The aim of this section is to provide a model of the selectivity filter and to compute the Hamiltonian H . In our model, the Hamiltonian is composed by three terms: the hydration energy, G_e , caused by the interaction of the ion with the surrounding water; the electrostatic component, H_e , between the ion and charged and polar groups within the channel; and an elastic component, H_c , associated to deformations of the channel shape. When a monovalent cation moves through the pore, it will polarize the surrounding medium (Andersen and Koeppel II, 1992). This induced

polarization, however, is the same for all alkali monovalent cations and cannot influence ionic selectivity. As a consequence, this electrostatic component will not be considered.

The elastic component

If x is a coordinate along the axes of the pore, the *shape* of the channel is defined by its *effective section* $\Sigma(x)$ at location x , so that the effective average radius is $R_o(x) = \sqrt{\Sigma(x)/\pi}$, as shown in Fig. 1 B. The assumption that channels have a cylindric section is done here only in order to simplify the calculations. Any channel shape, if explicitly known, could be easily included in the model. However, the effective section at the selectivity filter is likely to be more important than any specific geometry in determining the selectivity ratio. The channel can modify its shape because of the thermal motion of atoms composing the channel walls. Thus, it is unlikely that the channel radius remains fixed at its average value R_o . When the channel radius changes from its equilibrium value R_o to the new value R , an energy H_c is consumed. By expanding H_c in a Taylor series around its equilibrium value R_o and neglecting higher order terms, the following expression is obtained:

$$H_c(x) = 1/2 k(x) (R - R_o(x))^2. \quad (21)$$

where $k(x)$ is the elasticity coefficient of the channel radius at location x . This is equivalent to assuming that the channel radius $R_o(x)$ fluctuates with an r.m.s. σ of:

$$\sigma = \sqrt{\frac{RT}{k(x)}}. \quad (22)$$

The r.m.s. of polypeptide fluctuations can be evaluated both by experiments and numerical simulations and ranges from 0.05 Å to 1 Å for side chain atoms (Brooks III et al., 1988; Creighton, 1993).

Electrostatic components

The ion *interacts* with the charged or polar groups inside the channel. It is assumed that the ion and the site are *not in contact* and therefore they interact only by coulombic attraction or repulsion. This electrostatic interaction is screened by the dipoles surrounding the ion and the site and has the effective form:

$$H_e = \frac{e^2 z_s}{4\pi\epsilon(r)} \quad (23)$$

where $\epsilon(r)$ is a distance-dependent screening factor and z_s is the effective valence of charged and polar groups s . When r is large, $\epsilon(r)$ approaches the value of the macroscopic dielectric constant ϵ_w , but when r becomes small, the electric field becomes high enough to induce a saturation in the solvent's dipole orientation, thus leading to a lower value of $\epsilon(r)$.

This phenomenon is essentially a quantum mechanics effect and can be fully understood only by an *ab initio* approach. Within a semiquantitative approach it is possible to assume

that $\varepsilon(r)$ is calculated by Booth's model of dielectric saturation (Conway, 1981). In this case the dielectric constant, ε , in the presence of an electric field E is given by:

$$\varepsilon = \frac{\varepsilon_w - n^2}{b^{1/2}E} \arctan(b^{1/2}E) - n^2 \quad (24)$$

where n^2 is the square of the optical refractive index ($n^2 = 1.78$ for water), ε_w is the long-range limit of ε ($\varepsilon_w = 78$ for $T = 298$ K), $b = 1.08 \cdot 10^{-8} \text{ esu}^{-2}$, and E is the electric field, expressed in electrostatic units. Using $E = D/\varepsilon = e^2 z / 4\pi\epsilon r$, we obtain an equation for ε , which can be solved numerically. As shown in Fig. 3 A, the obtained solution saturates to ε_w for $r \approx 3.5 \text{ \AA}$. For small r , ε remains very close to $n^2 = 1.78$. As a consequence, when the distance between an alkali monovalent cation and a charged or polar group is $> 3.5 \text{ \AA}$, the electrostatic interaction is the same for a large and a small ion.

Hydration component

The last term of the Hamiltonian is the *hydration component*. At the selectivity filter a permeating ion has to lose some water molecules from its hydration shell, and it is necessary to estimate the *free energy* required for carrying the ion at position (x, r) inside the channel (see Fig. 1 B). Denoting by r_1 the ion radius and by r_w the (effective) radius of a water molecule (i.e., 1.4 \AA), it is evident that the center of a water molecule in contact with the ion can span a fraction $\Omega(x, r, R)$ of the sphere of radius $r_w + r_1$. This fraction is not 1, unless in bulk water, and depends on the position (x, r) of the ion: indeed some regions of the sphere are not accessible because of the presence of the channel walls (see Fig. 1 C). Given a pore geometry and ion position, Ω can be calculated explicitly; if the pore is locally cylindric, we have:

$$\Omega = \begin{cases} 1 & \Gamma - r > \rho; \\ 1 - \sqrt{1 - \left(\frac{\Gamma + r}{\rho}\right)^2} + \frac{1}{\pi} \int_{(\Gamma - r/\rho)}^{(\Gamma + r/\rho)} dt \frac{t}{\sqrt{1 - t^2}} \arccos\left(\frac{\Gamma^2 - r^2 - \rho^2 t^2}{2r\rho t}\right) & \text{for } \Gamma - r < \rho, \Gamma + r < \rho, \Gamma > r; \\ \frac{1}{\pi} \int_{(r - \Gamma/\rho)}^{(\Gamma + r/\rho)} dt \frac{t}{\sqrt{1 - t^2}} \arccos\left(\frac{-\Gamma^2 + r^2 + \rho^2 t^2}{2r\rho t}\right) & \text{for } \Gamma - r < \rho, \Gamma + r < \rho, \Gamma < r; \\ \frac{1}{\pi} \int_{(\Gamma - r/\rho)}^1 dt \frac{t}{\sqrt{1 - t^2}} \arccos\left(\frac{\Gamma^2 - r^2 - \rho^2 t^2}{2r\rho t}\right) & \text{for } \Gamma - r < \rho, \Gamma + r > \rho, \Gamma > r; \\ 1 - \frac{1}{\pi} \int_{(r - \Gamma/\rho)}^{(\Gamma + r/\rho)} dt \frac{t}{\sqrt{1 - t^2}} \arccos\left(\frac{-\Gamma^2 + r^2 + \rho^2 t^2}{2r\rho t}\right) & \text{for } \Gamma - r < \rho, \Gamma + r > \rho, \Gamma < r; \end{cases} \quad (25)$$

with $\Gamma = R(x) - r_w$ and $\rho = r_w + r_1$.

Neglecting the effect of secondary hydration shell, the hydration energy depends only on the number n_w of waters that can, on average, arrive in contact with the ion. Ω is introduced as a measure of n_w . In fact, on average, we have $n_w = 2 + (n_c - 2)\Omega$, where n_c is the primary coordination number of the ion (notice that this is, in general, a non-integer number) (see Table 2). As a consequence, for $R > r_w$, the minimum number of water molecules that can arrive in contact with the ion is 2, and if $\Omega = 1$ we have $n_w = n_c$.

We denote by G_i the free energy difference between the hydrated state, in which the ion is completely surrounded by molecules of water, and the state in which, as a result of the steric constraint, only i molecules of water are in contact with the ion (see Appendix B for details). When $\Omega = \Omega_i = i - 2/n_c - 2$ exactly i molecules of water are in contact with the ion, and $G_{\text{Hydr}}(\Omega_i) = G_i$. If $\Omega \in [\Omega_i, \Omega_{i+1}]$, i molecules of water are in contact with the ion, but they are not blocked by the walls and some secondary-shell waters get closer to the ion, without touching it. Thus, a *linear* dependence of G_{Hydr} on Ω is assumed:

$$G_{\text{Hydr}}(\Omega) = G_i + (G_{i+1} - G_i) \frac{\Omega - \Omega_i}{\Omega_{i+1} - \Omega_i}, \quad (26)$$

$$\Omega \in [\Omega_i, \Omega_{i+1}] i = 2, 3, \dots$$

When Ω is very small (i.e., equal to 0^+) the hydration free energy G_{Hydr} is equal to G_2 (see Fig. 1 B). When Ω increases, the ion and water molecules are not blocked in the channel and an entropic contribution is added (see Fig. 1 C). When Ω further increases, three or more water molecules can be in contact with the permeating ion (see Fig. 1 D).

The numerical values of the hydration free energies G_i used in our model are presented and discussed in Appendix C.

The effective Hamiltonian

In the model of the pore, the energy of a configuration in which the ion I is in position (x, r, θ) and the channel has a radius R , is

$$H^I(x, r, \theta, R) = 1/2 k(R - R_0(x))^2 + \sum_{s=1}^{\Sigma} H_c^I(r_{I,s}) + G_{\text{Hydr}}^I(\Omega^I(x, R, r)) \quad (27)$$

where, if (x_s, θ_s, R_s) is the position of site s , $r_{I,s} = \sqrt{(x - x_s)^2 + (r \cos(\theta - \theta_s) - R_s)^2}$. Equation 27 is the Hamiltonian of our problem, and, in the next section, we will use it for calculating permeability ratios. Two remarks on the form of the Hamiltonian of Eq. 27 are useful. The hydration energy in Eqs. 26 and 27 is described by a free energy and not by a simple potential energy, because the hydration of an ion involves many fast variables, which are likely to be thermalized on the time scale of the barrier crossing. As a consequence, the hydration energy is de-

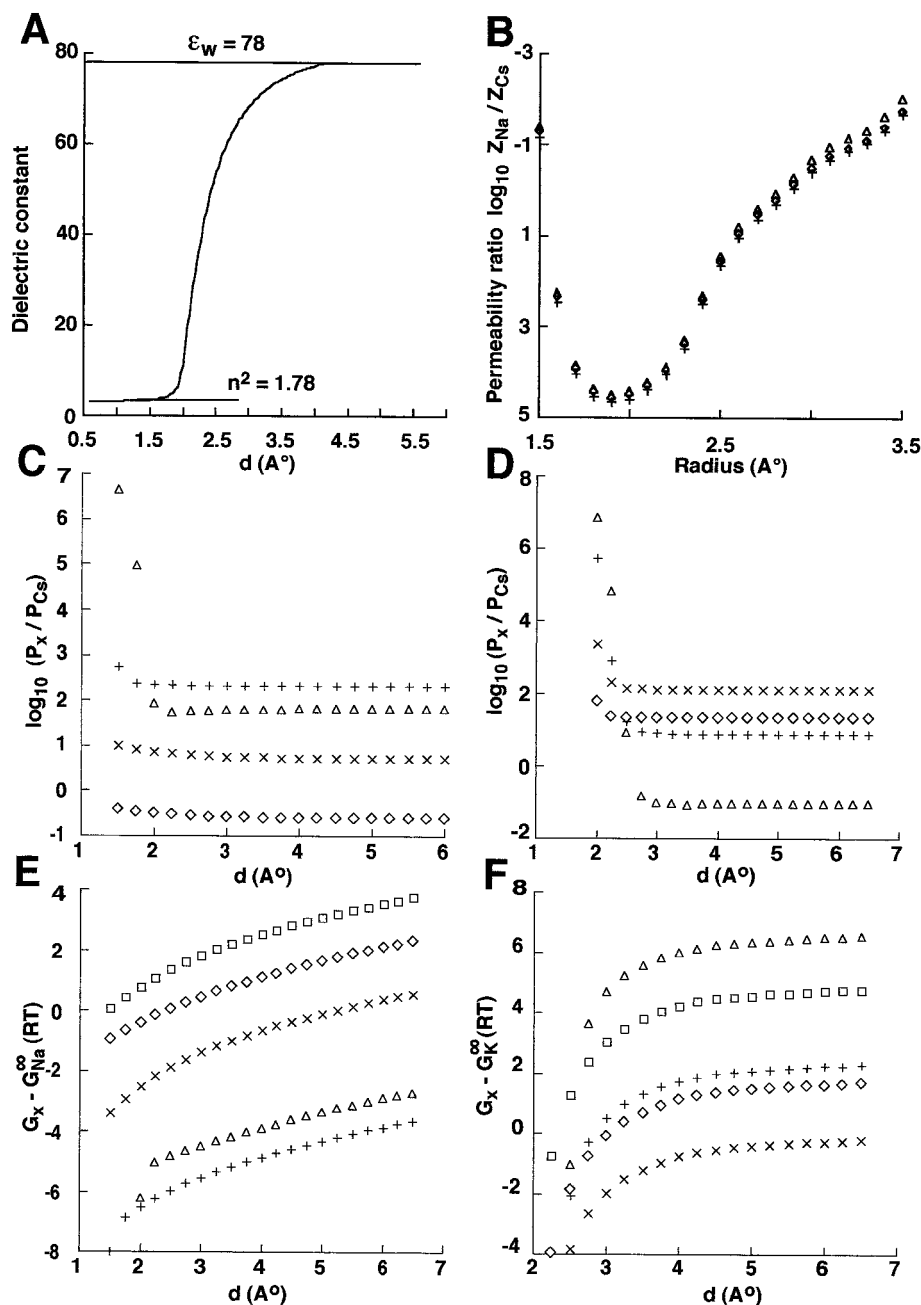


FIGURE 3 The role of electrostatic interactions in ionic selectivity. (A) The dependence of the dielectric constant ϵ on the distance between the ion and the charged site according to Eq. 24. (B) The ratio Z_{Na}/Z_{Cs} as a function of channel radius in the absence of charged and polar sites (+) and in the presence of two charges of charge $-e$, with effective radius 1 Å, and located 2 Å from the selectivity filter (Δ) and four charged sites of charge e with an effective radius of 1 Å located 2 Å from the selectivity filter (◇). (C) Permeability ratios P_x/P_{Cs} as a function of distance d between the selectivity filter and four charges of charge $-e$. Two charges are at $-d$ with angular position 0 and π and two charges are at d with angular position $\pi/2$ and $3/2\pi$. Channel radius of 3 Å with no fluctuations. (D) as in (C) but in the presence of two rings of four dipoles at a distance d from the selectivity filter (one ring at $+d$ and one ring at $-d$). Each dipole is composed by two charges of $\pm 0.42e$ at a distance of 1.1 Å at the angular location of 0, $\pi/2$, π , and $3/2\pi$. In (C) and (D) permeability ratios for Li^+ (Δ), Na^+ (+), K^+ (×), and Rb^+ (◇). Channel radius is 1.5 Å fluctuating with an r.m.s. of 0.05 Å. In (E) and (F) Gibbs free energies are scaled to the Gibbs free energy of Na^{+} in the absence of electrostatic interactions G_{Na}^{∞} (G_K^{∞}) for Li^+ (Δ), Na^+ (+), K^+ (×), Rb^+ (◇), and Cs^+ (□) as a function of the distance d between the selectivity filter and charged (E) or polar (F) groups for the configurations described in (C) and (D), respectively.

scribed by a free energy that takes into account these degrees of freedom. On the contrary, the deformation of the channel radius, involving the displacement of a large number of atoms, occurs on a slower time scale and therefore is

not averaged during barrier crossings. These deformations lead to variable permeability ratios, which are subsequently averaged on the time scale of electrophysiological experiments involving a large number of barrier crossings.

TABLE 1 Enthalpies and entropies in the gas phase (from Kebarle, 1974)

| Ion | 0,1 | 1,2 | 2,3 | 3,4 | 4,5 | G_{hydr} |
|---------------|--------------------------|----------|----------|------------|--------------|-------------------|
| Li^+ | 34* 23 [#] | 26 21 | 21 25 | 16 30 | 14 31 | 119.61 |
| Na^+ | 24* 21.5 [#] | 20 22 | 16 22 | 14 25 | 12 28 | 95.73 |
| K^+ | 18* 21.6 [#] | 16 24 | 13 23 | 12 25 | 11 25 | 78.08 |
| Rb^+ | 16* 21 [#] | 14 22 | 12 24 | 11 25 | 10 25 | 73.01 |
| Cs^+ | 14* 19.4 [#] | 12 22 | 11 24 | 10.6 25 | n.a. n.a. | 65.3 |

$i, i + 1$ refers to the binding of a water molecule to an ion with i water molecules already bound. G_{hydr} is the hydration energy in the liquid phase of the different ions. n.a., not available.

*Enthalpies in kcal M^{-1} .

[#]Entropies in $\text{cal M}^{-1} \text{K}^{-1}$.

It is now possible to summarize the obtained theoretical results. The permeability ratio between ion A and B is given by Eq. 6, where, given our model of the pore, we have

$$\begin{aligned}
 G_i(x) &= -\frac{1}{\beta} \ln Z_i \\
 &= -\frac{1}{\beta} \ln \left[\int d\theta \int dR \int dr r \exp(-\beta H^i(x, r, \theta, R)) \right] \\
 &= -\frac{1}{\beta} \ln \left[\int d\theta \int_{r_1}^{+\infty} dR \int_0^{R-r_1} dr r \right. \\
 &\quad \cdot \exp \left(-\beta \frac{1}{2} k(R - R_0(x))^2 \right. \\
 &\quad \left. \left. + \sum_{s=1}^{\infty} H_c^i(r_{1,s}) + G_{\text{Hydr}}^i(\Omega^i(x, R, r)) \right) \right] \quad (28)
 \end{aligned}$$

and where τ_B/τ_A is the diffusive correction, given by Eq. 18. The integrals in Eq. 28 were computed by standard numerical routines.

TABLE 2 Parameter alkali values used for cations

| Parameter | Li^+ | Na^+ | K^+ | Rb^+ | Cs^+ |
|---|---------------|---------------|--------------|---------------|---------------|
| D ($\text{cm} \cdot \text{s}^{-2}$) $\cdot 10^{-5}$ | 1.03 | 1.33 | 1.96 | 2.07 | 2.06 |
| r_1 (\AA) | 0.6 | 0.95 | 1.33 | 1.49 | 1.65 |
| n_c | 4.9 | 6.8 | 7.7 | 8.2 | 9.3 |
| G_2 kcal mol^{-1} | 25.84 | 22.74 | 19.89 | 19.53 | 16.98 |
| G_3 | 12.27 | 13.57 | 14.13 | 15.11 | 13.67 |
| G_4 | 4.77 | 6.99 | 9.67 | 11.72 | 10.78 |
| G_5 | -0.86 | 2.99 | 5.94 | 9.06 | — |

D is the diffusion constant, r_1 is the atomic radius, n_c is the coordination number. G_i is the value obtained from Eq. B.6 of the hydration free energies in the liquid phase.

COMPARISON WITH EXPERIMENTAL RESULTS

In this section we will see that the selectivity sequence of the majority of monovalent cationic channels can be explained by Eqs. 6 and 28 for appropriate values of R_0 and k , without any relevant contribution from electrostatic interaction with charged or polar groups. In the next section it is shown that the effect of charged and polar groups on P_B/P_A between ions with the same valence is small, *unless the ion is in contact with a charged or polar group at the selectivity filter*. This last possibility has already been discussed in details in the literature and it will not be considered here. The present theory will reduce to an Eisman-like theory if a van der Waals contact with a charged or polar group at the selectivity filter is assumed. However, it is important to observe that the selectivity ratio is primarily determined by the highest barrier of the Gibbs free energy profile. Indeed, the most unfavorable location for the ion inside the channel (i.e., the highest barrier) is expected to be the region *between* two charged and polar groups and not a region in which it is in contact with them.

Thus, if a certain distance between the selectivity filter and charged or polar residues is assumed, the only relevant microscopic parameters of the proposed theory are R_0 and k . The effect on P_B/P_A of changing their values over a plausible range is shown in Figs. 4 and 5. In subsequent sections the selectivity of K^+ , gramicidin, Na^+ , cyclic nucleotide gated (CNG), and end plate channels will be discussed in more detail.

Fig. 4 *A* reproduces the permeability ratios relative to Cs^+ for the monovalent cations Li^+ (Δ), Na^+ ($+$), K^+ (\times), and Rb^+ (\diamond) as a function of the channel radius obtained from Eqs. 6 and 28. The value of the parameter k was $200 \text{ kcal} \cdot \text{\AA}^{-2}$, corresponding to fluctuations in the channel radius with a r.m.s. of 0.053 \AA . It is evident that several different selectivity sequences are present for increasing radii:

1. For pore radius $\sim 1.50 \text{ \AA}$ the selectivity sequence is $\text{K}^+ > \text{Rb}^+ > \text{Cs}^+ > \text{Na}^+ > \text{Li}^+$, identical to the selectivity sequence of K^+ channels;
2. For pore radius $\sim 2 \text{ \AA}$ the selectivity sequence becomes $\text{Cs}^+ > \text{Rb}^+ > \sim \text{K}^+ > \text{Na}^+ > \text{Li}^+$, identical to the selectivity sequence of gramicidin channels;
3. For pore radius $\sim 2.6 \text{ \AA}$ the selectivity sequence is $\text{Na}^+ \approx \text{Li}^+ > \text{K}^+ > \text{Rb}^+ \approx \text{Cs}^+$, reminiscent of that found in Na^+ channels;
4. For radius $\sim 4 \text{ \AA}$ the channel becomes poorly selective, as in CNG channels;
5. For radius $> 4 \text{ \AA}$ the selectivity sequence becomes again $\text{Cs}^+ > \text{Rb}^+ > \text{K}^+ > \text{Na}^+ > \text{Li}^+$, as in end plate channels.

Thus, Eqs. 6 and 28 are able to predict the relevant selectivity sequences found in monovalent cation channels. Fig. 4, *B* and *C* reproduces the permeability ratios relative to Cs^+ for smaller values of the parameter k corresponding to larger fluctuations in the channel radius (in Fig. 4, *B* and *C* the r.m.s. is 0.17 \AA and 0.38 \AA , respectively). The selectiv-

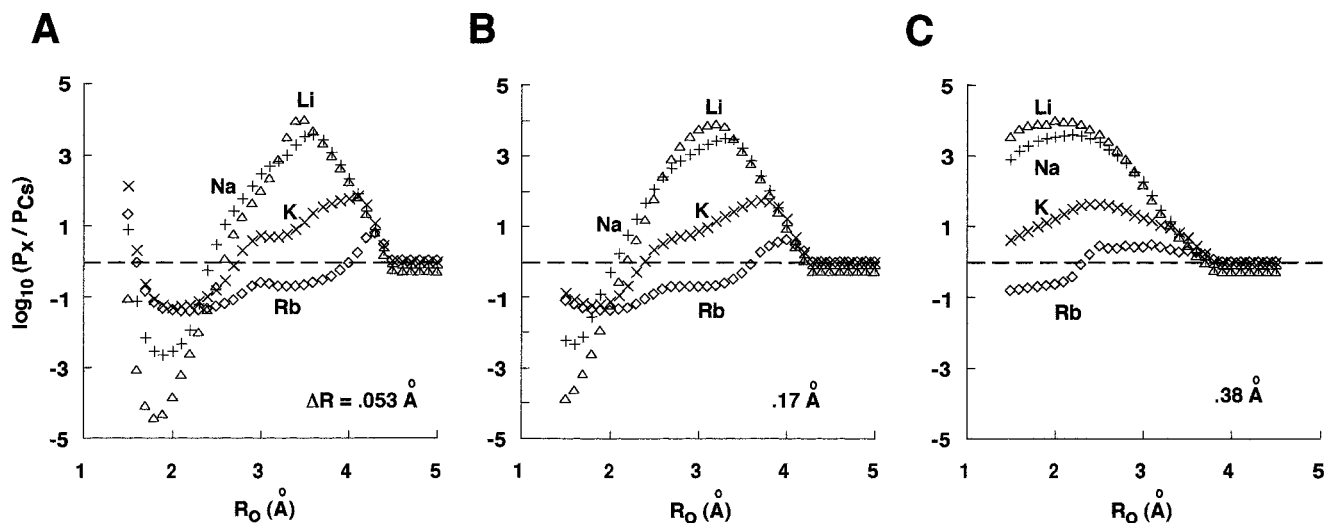


FIGURE 4 The permeability ratio P_x/P_{Cs} as a function of channel radius R_0 with a value of 0.053 Å (A), 0.17 Å (B), and 0.38 Å (C) for the r.m.s. of radius fluctuations for Li^+ (Δ), Na^+ ($+$), K^+ (\times), and Rb^+ (\diamond).

ity sequences are the same as those observed with a more rigid channel (compare Fig. 4 A), but a specific sequence is obtained for a smaller value of R_0 . In the presence of significant fluctuations of R_0 , barrier crossings preferentially occur during a fluctuation corresponding to a large value of R_0 , when the ion can permeate with more water molecules attached. In this regime, the ion prefers to wait for a large fluctuation so that it can cross the barrier in a more hydrated configuration. The selectivity sequences obtained for different values of R_0 and k are summarized in Table 3.

Charged and polar groups and ionic selectivity

This section contains a discussion of the role of charged and polar groups near the selectivity filter in the determination of the selectivity of the channel among ions with the same valence. By using Eq. 23 for ion-charged group interactions, the ratio Z_A/Z_{Cs} can be computed for the monovalent cations

for different site configurations around the selectivity filter. Fig. 3 B reproduces Z_{Na}/Z_{Cs} computed for a channel without charged or polar groups ($+$), with two charged groups of charge $-e$, and effective radius 1 Å, located 2 Å from the selectivity filter (Δ) and with four charged groups of effective radius 1 Å, located 2 Å from the selectivity filter (Δ) and with four charged groups of effective radius 1 Å, located 2 Å from the selectivity filter (two at each side) in the configuration minimizing the group-group interaction (\diamond). Let us also consider two configurations of charged and polar groups that can be found in ionic channels: two pairs of carboxyl groups (Fig. 3, C and E) such as those of aspartic and glutamic acids, and two rings of four dipoles (Fig. 3, D and F) similar to carboxyl groups of the protein backbone. Fig. 3 C reproduces permeability ratios for a rigid channel with a radius R_0 equal to 3 Å in the presence of four elementary charges with a van der Waals radius of 1.4 Å at a variable distance d from the selectivity filter. When charges are located at a distance >2 Å the permeability ratios are hardly affected by electrostatic interactions. Fig. 3 D illustrates a similar result in the case of four polar groups at each side of the selectivity filter. The dipole of these groups is modeled by two charges of $\pm 0.42e$ at a distance of 1.1 Å, as for the carbonyl group of the protein backbone. In this case the channel has a radius of 1.5 Å fluctuating with a r.m.s. of 0.05 Å. As in the case illustrated in Fig. 3 C, electrostatic interactions do not affect permeability ratios when the polar groups are at a distance >2.5 Å from the selectivity filter. In the configuration of Fig. 3 C, with $d = 2.5$ Å, we also checked that P_B/P_A is almost unaffected when the angular position of the two charged groups at the left of the selectivity filter was varied. When the distance between the selectivity filter and charged and polar groups is below 2 Å, the barrier of the selectivity filter coalesces into the binding sites and the proposed theory does not hold;

TABLE 3 Selectivity sequences as function of R_0 and σ

| R_0 (Å) | 0.053 | 0.17 | 0.36 σ (Å) |
|-----------|-------|-------|-------------------|
| 1.5 | K_1 | K_2 | L_2 |
| 2 | G | G | L_2 |
| 2.5 | Na | Na | L_1 |
| 3 | Na | L_1 | CNG |
| 3.5 | L_1 | CNG | CNG |
| 4 | CNG | D | D |
| >4 | D | D | D |

Selectivity sequences obtained for different channel radii R_0 fluctuating with an r.m.s. σ . The selectivity sequences are: $K_1 = (K^+ > Rb^+ > Cs^+ > Na^+ > Li^+)$; $K_2 = (K^+ \approx Cs^+ > Rb^+ > Na^+ > Li^+)$; $G = (Cs^+ > Rb^+ \approx K^+ > Na^+ > Li^+)$; Na = ($Na^+ \approx Li^+ > K^+ > Rb^+ \approx Cs^+$); $L_1 = (Li^+ > \sim Na^+ > K^+ > Rb^+ > Cs^+)$; $L_2 = (Li^+ > Na^+ > K^+ > Cs^+ > Rb^+)$; CNG = ($Na^+ \sim K^+ > Li^+ > Rb^+ > Cs^+$); $D = (Cs^+ > \sim Rb^+ > \sim K^+ > \sim Na^+ > \sim Li^+)$.

a full simulation of molecular dynamics is then more adequate.

These results and several other simulations indicate that there exists a large class of channels in which *the presence of charged and polar groups changes the selectivity properties of the channel only slightly*. Moreover, as it will be shown below, this class is wide enough to provide all the important selectivity sequences found in usual channels.

The reason for this behavior is that if a small ion such as Li^+ and a large ion such as Cs^+ interact with charged and polar groups located at some distance, the coulombic interaction will be the same for the large and small ion. As a consequence, the difference in the Gibbs free energy at the selectivity filter between a small ion (such as Li^+) and a large ion (such as Cs^+) will be almost identical in the presence or in the absence of charged and polar groups. The screening factor ϵ_w in Eq. 23 will obviously depend on the quantity of water between the ion and the charged and polar groups, and this does depend on the size of the ion; but, in the range of ion-site distance considered here, this is a second-order effect.

What is, then, the role of charged and polar groups in ionic channels? An answer to this question can be obtained by analyzing the effect of electrostatic interactions on the absolute height of the barrier at the selectivity filter. This is shown in Fig. 3, *E* and *F* for the two configurations considered in Fig. 3, *C* and *D*, respectively. In Fig. 3, *E* the Gibbs free energy of the different ions minus the Gibbs free energy for Na^+ in the absence of electrostatic interactions is plotted as a function of the distance d . Similarly, in Fig. 3, *F*, the reference Gibbs free energy is that of K^+ . It is evident that stronger electrostatic interactions decrease the Gibbs free energy, but almost similarly for all the monovalent cations. As expected, the role of electrostatic interactions decays more rapidly in the case of dipoles (see Fig. 3, *F*) than in the case of electric charges (see Fig. 3, *E*).

The activation energy of permeating ions ranges between 8 and 15 RT, while the free energy necessary to remove all the water molecules of the hydration shell with the exception of two or three from hydrated monovalent cation varies between 25 and 80 RT. As a consequence, during ionic permeation the free energy barrier must be significantly reduced by the presence of catalytic agents, most likely charged and polar groups, as observed in molecular dynamics simulations (Roux and Karplus, 1993). Thus, the role of charged and polar groups is crucial in the determination of the value of ionic currents through the channel and the selectivity ratio between ions of different valence, but not the selectivity ratio between ions with the same valence.

The contribution of τ_B/τ_A to permeability ratios

The permeability ratios shown in Fig. 4 were obtained using Eq. 18 for estimating τ_B/τ_A . It is important to see the effect of using a different equation for the ratio τ_B/τ_A on the computed permeability ratios, i.e., when τ_B/τ_A is given by Eq. 18, Eq. 14, or when it is equal to 1. In the three cases the permeability ratios are very similar, indicating that the ma-

ior determinant of the permeability ratio is the free energy component and not the term τ_B/τ_A .

K^+ channels

Potassium channels are usually permeable only to a very limited number of ions, such as K^+ , Rb^+ , NH_4^+ , Ti^+ , and Cs^+ . The permeability of Cs^+ through K^+ channels varies in different channels and can be as high as 0.18 in the delayed rectifier of snail neurons (Reuter and Stevens, 1980) and <0.03 in the inward rectifier of starfish eggs (Hagiwara and Takahashi, 1974); K^+ channels are not permeable to larger organic molecules and their radius has been estimated to be between 1.48 and 1.65 Å, in agreement with the prediction shown in Fig. 1 *A*. Equations 6 and 28 can also explain the different permeability ratios for Cs^+ found in different K^+ channels. Fig. 5 illustrates the permeability ratio relative to K^+ for Li^+ (○), Na^+ (□), Rb^+ (◇), and Cs^+ (△) as a function of the parameter k with an average radius of 1.5 Å. It is evident that different Cs^+ permeabilities can be quantitatively accounted for by different fluctuations of the pore radius: a larger Cs^+ permeability is associated to larger fluctuations. The selectivity of the delayed rectifier ($P_{\text{Rb}}/P_{\text{K}} = 0.74$, $P_{\text{Cs}}/P_{\text{K}} = 0.18$, $P_{\text{Na}}/P_{\text{K}} = 0.07$, and $P_{\text{Li}}/P_{\text{K}} = 0.09$) is quantitatively obtained for fluctuations corresponding to an elastic coefficient of 60 kcal/Å², while the selectivity of the inward rectifier ($P_{\text{Rb}}/P_{\text{Cs}} = 0.35$ and <0.03 for $P_{\text{Cs}}/P_{\text{K}}$ and $P_{\text{Na}}/P_{\text{K}}$) is obtained with a value for k of ~ 87 kcal/Å².

The selectivity of K^+ channels can be intuitively explained by a combination of steric and energetic factors. If the channel pore is ~ 1.5 Å, Li^+ , Na^+ , and K^+ can permeate through it with two water molecules at the two sides of the

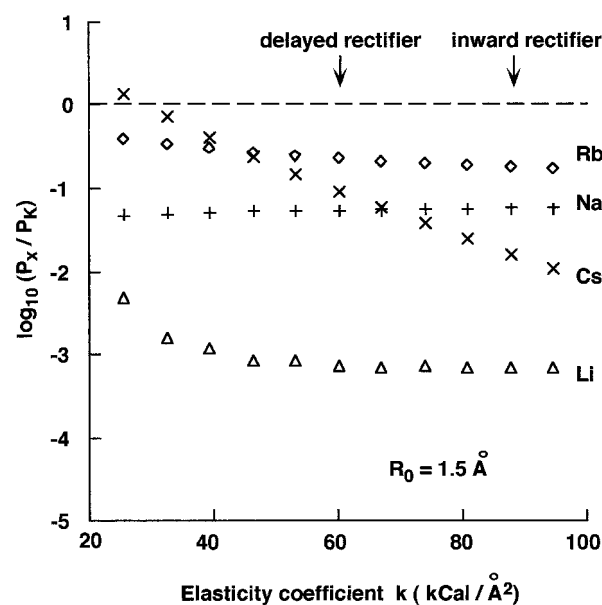


FIGURE 5 The permeability ratio P_x/P_K as a function of the elastic coefficient k for Li^+ (△), Na^+ (+), Rb^+ (◇), and Cs^+ (×), respectively, with a value of 1.5 Å for R_0 .

pore (see Fig. 1, *B* and *C*). Large alkali cations such as Cs^+ are excluded from K^+ channels because they are too large to permeate easily. Small cations such as Li^+ and Na^+ do not permeate as well as K^+ through K^+ channels because of energetic factors: the energy required to remove all water molecules except two is much larger for Li^+ and Na^+ than for K^+ . The free energy cost of removing all the water molecules except two is very large and a substantial “catalytic” effect is required to lower the barrier. This catalytic effect may be provided by the ring of negatively charged aspartate commonly found in K^+ channels (Kirsch et al., 1995; Lipkind and Fozzard, 1995).

Gramicidin channels

The radius of gramicidin channels is ~ 2 Å (Wallace, 1990), and their selectivity sequence is $\text{Cs}^+ > \text{Rb}^+ > \sim \text{K}^+ > \text{Na}^+ > \text{Li}^+$ (Myers and Haydon, 1972). This selectivity sequence is well predicted by Eqs. 6 and 28 for a channel radius of ~ 2 Å and can be explained by observing that in the gramicidin channel all alkali cations Li^+ , Na^+ , K^+ , Rb^+ , and Cs^+ can permeate through it with two water molecules attached at the two sides of the pore (as shown in Fig. 1 *C*). As a consequence, the selectivity sequence is primarily determined by energetic factors, favoring larger cations such as Cs^+ .

Na^+ channels

Sodium channels are permeable also to small organic compounds such as formamidinium, guanidinium, and aminoguanidinium; their pore has been estimated to be a rectangular slit of 3.1×5.1 Å (Hille, 1992) and their selectivity sequence is $\text{Na}^+ \sim \text{Li}^+ > \text{K}^+ > \text{Rb}^+ > \text{Cs}^+$. This selectivity sequence is predicted by Eqs. 6 and 28 for a channel radius of ~ 2.6 Å or more. The area of a slit of 3.1×5.1 Å is the same as that of a circular section of radius 2.25 Å, which is in some agreement with the value of 2.6 Å corresponding to a selectivity sequence close to that observed in Na^+ channels.

Qualitatively, the selectivity sequence of Na^+ channels originates because small ions such as Li^+ and Na^+ can permeate through it with three water molecules (as shown in Fig. 1 *D*), but not larger cations such as K^+ , Rb^+ , and Cs^+ . In fact, for Li^+ and Na^+ $2(r_w + r_i)$ is 4.2 Å and 4.9 Å (hence smaller than 5.1 Å), while for K^+ , Rb^+ , and Cs^+ it is 5.46 Å, 5.76 Å, and 6.1 Å, respectively; this qualitative behavior is reproduced, in our model, for $R_0 > 2.6$ Å. As a consequence, its selectivity is determined by steric and energetic factors.

CNG channels

CNG channels are slightly larger than Na^+ channels, as methylamine is permeable through CNG channels but not through Na^+ channels (Picco and Menini, 1993) and their dimensions at their narrowest restriction have been esti-

mated to be 5.1×3.6 Å. Native CNG channels are poorly selective among monovalent cations and have the following selectivity sequence: $\text{Li}^+ > \text{Na}^+ > \text{K}^+ > \text{Rb}^+ > \text{Cs}^+$ (Menini, 1990). According to Eisenman (1962) this selectivity sequence would be caused by strong electrostatic interactions within the pore. However, it has been shown that entropic contributions determine the selectivity of Li^+ over Na^+ (Sesti et al., 1996). The selectivity sequence of the alpha subunit of the CNG channel is $\text{Na}^+ \sim \text{K}^+ > \text{Li}^+ > \text{Rb}^+ > \text{Cs}^+$ and is not modified when negative charges within the pore are neutralized (Eismann et al., 1994; Sesti et al., 1996), but the single channel conductance is reduced by at least 10 times (Sesti, Nizzari and Torre, unpublished observations). CNG and Na^+ channels have the same selectivity sequence but $P_{\text{Cs}}/P_{\text{Na}}$ is ~ 0.01 in Na^+ channels and 0.6 in CNG channels. This different quantitative behavior can be explained if CNG channels have an average radius of ~ 3 Å and an r.m.s. of radius fluctuations of 0.38 Å or more (see Fig. 4 *C*). Under these conditions small ions such as Li^+ and Na^+ can permeate with almost their entire first hydration shell. In this case the permeability ratio is determined by the frequency of these events, which is larger for small cations like Na^+ and Li^+ .

End plate channels

End plate channels are permeable to a variety of organic compounds such as urea and triethylammonium, and their estimated radius is ~ 3.5 Å (Dwyer et al., 1980). Their selectivity sequence is $\text{Cs}^+ > \text{Rb}^+ > \text{K}^+ > \text{Na}^+ > \text{Li}^+$. This selectivity sequence is obtained when P_B/P_A approaches D_B/D_A , when ions move through the channel almost in a fully hydrated configuration.

In our model, the diffusive regime is reached when ions cross the channel with all their primary hydration shell. The diffusive regime is reached for channel radii larger than 3.5 Å for Li^+ , Na^+ , and K^+ , and only when R_0 is greater than 4.3 Å for Cs^+ . If the channel radius is 3.5 Å, Cs^+ can cross it with 6–7 water molecules in the primary hydration shell, while its primary coordination number is ~ 9 (see Table 2). The selectivity sequence of end plate channels, which is very similar to that observed for a simple diffusion in water, indicates that Cs^+ may permeate in its fully hydrated configuration also through a channel with a radius of ~ 3.5 Å, corresponding to a value of Ω significantly smaller than 1. This state can be reached when water molecules pack around the ions and a fully hydrated configuration may be reached also if $\Omega < 1$. This “packing” of water around the ion is not kept into account by our model, and can be fully described only within a molecular dynamics approach.

DISCUSSION

The goal of this manuscript is to provide a theoretical analysis of the physical origin of selectivity among monovalent alkali cations of ionic channels in biological membranes and to discuss recent experimental results in the light

of this analysis. The essence of this theoretical analysis is the derivation of Eqs. 6 and 28 relating the permeability ratio P_B/P_A to physical properties of the channel and to the thermodynamics of ion hydration. The major implication of these equations is that the ionic selectivity among monovalent alkali cations, found in K^+ , gramicidin, Na^+ , CNG and end plate channels, can be explained by simple geometrical properties of the channel. In this view electrostatic interactions between the permeating ion and charged and/or polar residues within the channel determine the single channel conductance and catalyze the ionic transport through the channel (see section on Charged and Polar Groups above). On the contrary, ionic selectivity is primarily controlled by channel geometry (see Fig. 4).

Range of validity of the proposed approach

The theoretical approach to ionic selectivity proposed in this paper is primarily based on the assumption of describing the ionic permeation by a single reaction coordinate $x(t)$ obeying to a Langevin equation with a term describing the Gibbs free energy $G(x)$. These assumptions are equivalent to having a clearcut separation between the different time scales of the system under consideration: the time scale on which an ion permeates through the selectivity filter τ_b must necessarily be larger than the time scale of fast molecular motion τ_f and shorter than the time scale of slow molecular motion τ_s . When $\tau_f \ll \tau_b$ it is possible to assume that thermalization occurs over the fast variables and to have a well-defined $G(x)$. When $\tau_b \ll \tau_s$ it is possible to consider as parameters the slow moving variables x_s and to parametrize the Gibbs free energy $G(x, x_s)$, and finally to average the results over the slow variables x_s . As the crossing of the selectivity filter occurs in a time scale between 10 and 100 ns, all the dynamics occurring in the ps range, such as water interactions, bond vibrations, and fast molecular motions, are described by fast variables assumed in thermal equilibrium. Slow motions of the channel occurring in the microsecond range, leading for instance to changes of the channel radius, can be described as parameters. The proposed approach should be reconsidered when several variables have a characteristic time scale comparable to τ_b . This will be the case when residues constituting the selectivity filter fluctuate with a period comparable to τ_b . In this case more complex multidimensional Langevin equations must be considered.

Another important assumption of the proposed approach is that the highest barrier of the Gibbs free energy is at some distance from binding sites, i.e., from charged and polar groups. This assumption should be weakened if a very detailed and quantitative description of channels such as gramicidine was required. Indeed, molecular dynamics simulations of the permeation through gramicidin channels (Roux and Karplus, 1991, 1993, 1994) have shown that at the barriers of the Gibbs free energy the ion still remains in contact with a backbone carbonyl group.

The proposed theory also assumes that interactions between permeating ions are not essential in determining ionic selectivity. The justification for this simplifying assumption is that selectivity does not change significantly when the concentration of permeating ions is reduced so that at any time at most one ion is present in the channel (see the Permeability Ratio section) and ion-ion interactions can be neglected.

The proposed approach also considers two important aspects of ionic permeation, i.e., friction and diffusion, which were not considered in many previous approaches (see the first section), but only in a few papers (Cooper et al., 1988a, b; Andersen, 1989); their relevance in ionic permeation has often been neglected.

The role of charged and polar groups

An important conclusion of the proposed theory is that charged and polar groups in the channel are not the major determinants of ionic selectivity among ions with the same valence, but act primarily as catalysts for ionic permeation (see above). These conclusions are based on Eqs. 7 and 10, which imply that ionic selectivity primarily depends on the height of the highest barrier and very weakly on well depths. These results indicate that the selectivity filter is located between two neighboring wells, where the permeating ion interacts with charged and polar groups. As a consequence, the selectivity filter is located at some distance from these groups and the electrostatic interactions experienced by monovalent alkali cations will be almost identical (see The Elastic Component and The Effective Hamiltonian). Electrostatic interactions are crucial for the selectivity among cations versus anions (Roux, 1996; Dorman et al., 1996) and among monovalent versus divalent cations (Heinemann et al., 1992; Kim et al., 1993; Yang et al., 1993). A major role of charged and polar groups is to catalyze the dehydration process and thus to determine the absolute flux over the selectivity barrier, i.e., to control the single channel conductance.

Dependence on the experimental values of hydration free energy and ionic radii

The numerical values of the permeability ratios P_B/P_A obtained in Fig. 4 depend on the values used for computing the hydration free energy, as discussed in Electrostatic Components and Appendix B. The values used here are those experimentally measured by Kebarle (1974) and Blades et al. (1990) and are similar within 10% to other values reported in the literature. The numerical values of hydration energy are also similar within 10% to the computed values for ion-water cluster ab initio simulations recently obtained (Glendening and Feller, 1995; Rananich, Bernasconi, and Parrinello, submitted for publication). No comparison between the values experimentally measured and those obtained by molecular dynamics is available for the entropic contribution. The values reported by Kebarle (1974) were

obtained with the same experimental technique for the five monovalent cations considered here, and were chosen for this reason. P_B/P_A depends also on the numerical values of ionic radii r_i . The set of Pauling radii is used here. The use of different experimental values will influence the quantitative permeability ratios, but not the general trend observed in Fig. 4.

Limitations of the proposed theory

The selectivity sequences predicted by the proposed approach and illustrated in Fig. 4 do not conform exactly (i.e., quantitatively) to those observed experimentally in biological channels. Although the predicted sequence is often qualitatively correct, the exact permeability ratios are often too large. This is the case for the gramicidin channel and for the Na^+ channel. In addition, the permeability ratio between Rb^+ and Cs^+ is <1 for channel radii between 2.4 and 4 Å, while in Na^+ and CNG channels this ratio is >1 . Similarly, the permeability ratio between Rb^+ and K^+ is <1 for channel radii ~ 2 Å, while it is >1 in the gramicidin channel. These discrepancies most likely have two origins. First, the presence of charged and polar groups, not considered in the calculations illustrated in Fig. 4; second, the uncertainty on the numerical values of hydration energies. In the case of the gramicidin channel the selectivity filter is expected to be quite near the different dipoles present in the channel, probably at a distance of <2 Å, when the proposed approach becomes unsatisfactory. In addition, the entropic contributions for adding a water molecule to Rb^+ and Cs^+ were measured more than 20 years ago (Kearle, 1974) and these values were never compared with those obtained from molecular dynamics simulations (see above).

The proposed theory aims at describing a molecular process, such as the ionic permeation in a classical framework of statistical mechanics. As a consequence, basic molecular interactions are neglected and their functional role is lost. For instance, the interaction between water molecules and the permeating ion is described in a rather empirical way, while a molecular dynamics approach is more appropriate, especially when the second hydration shell becomes relevant, which is neglected here. This is the case of the permeation through large channels, such as the CNG and end plate channels, where ions are likely to permeate with a significant water shell. The interaction of the permeating ion and charged and polar groups at distances shorter than 2.5 Å is likely to involve significant changes in the electronic state. These events can only be captured by ab initio simulations, requiring a quantum mechanical approach.

Predictions and conclusions

The proposed explanation of ionic selectivity can be tested by verifying some predictions. First, it is predicted that by changing the electrical charges and the dipoles within the pore region, no major change of ionic selectivity will occur.

It is difficult to summarize all the results of experiments on site-specific mutagenesis on the role of charged and polar groups in the determination of ionic selectivity, but some general remarks can be made. When amino acids in the putative pore region of K^+ channels are mutated, the permeability ratio between K^+ and Na^+ can be reduced or unselective channels can be obtained (Heginbotham et al., 1994; Kirtsch et al., 1995) but it has not yet been possible to transform a K^+ channel into a Na^+ channel by changing charged and/or polar residues. Similarly, it is possible to reduce the permeability ratio between Na^+ and K^+ (Faure et al., 1996) but not to transform a Na^+ into a K^+ channel. These results support the notion presented in this paper that ionic selectivity is not primarily determined by electrostatic interactions.

The proposed theory predicts that in order to transform a K^+ channel into a Na^+ channel it is necessary to increase the radius of the pore, which can be obtained by molecular engineering techniques. The permeation of large organic cations can be used to probe the pore radius and verify changes of the pore radius. The observation that *shaker* K^+ channels during C-type inactivation becomes permeable to Na^+ (Starkus et al., 1997) could be explained as produced by an increase in the pore radius.

The proposed theory provides some additional predictions on the structure and function relation of ionic channels. For instance, K^+ channels have a variable value of $P_{\text{Cs}}/P_{\text{K}}$ and it is predicted that K^+ channels with a large Cs^+ permeability are more flexible than those with a low Cs^+ permeability (see Fig. 5). K^+ channels with a sharp selectivity are expected to have a rather rigid diameter at the selectivity filter of ~ 3 Å. It is also predicted that CNG channels have a significant pore flexibility and that the major difference in the pore region between CNG channels and voltage gated channels (Na^+ and K^+ channels) is the extent of residues motion, which is larger in CNG channels.

The theoretical approach proposed in this paper aims at explaining selectivity in ionic channels of biological membranes without considering the specific amino acid composition of the channel. Different channels are simply characterized by two parameters, i.e., the pore radius R_0 and the r.m.s. of its fluctuations. The proposed theory provides an explanation for two fundamental observations on ionic selectivity: first, why K^+ channels have a narrow pore with a radius of ~ 1.5 Å and Na^+ channels are larger; second, why ionic selectivity and single channel conductance are independent features of ionic channels.

In its simplicity, the proposed theory seems to capture the essence of selectivity of monovalent cationic channels and it will be interesting to see whether the proposed approach can be extended to divalent cationic channels and to anionic channels. More accurate characterizations of permeation through the various channels will require a detailed molecular description of the channel, a real dynamical treatment of the process, and possibly a quantum mechanical approach to chemical interactions with charged and polar groups.

APPENDIX A

This appendix will briefly review some properties of Langevin equation and Kramer rate theory. A fundamental hypothesis usually made in KRT is the existence of a large gap between the time scales required for the barrier crossing and all the other relevant time scales of the system dynamics. Under these conditions, it is possible to write down an equation for a (macroscopic) reaction coordinate $x(t)$ describing the transition of the system by simply taking an average with respect to the other degrees of freedom, thus obtaining a reduced description from the full phase space to the reaction coordinate space. This equation has a Langevin form

$$M\ddot{x} + \frac{dG}{dx} + M\gamma\dot{x} = \xi(t) \quad (\text{A.1})$$

where $G(x)$ is the mean field potential, here referred to as the Gibbs free energy, depending on the reaction coordinate x , $\xi(t)$ is a thermal noise, and γ is a friction satisfying the fluctuation-dissipation theorem (Hanggi et al., 1990)

$$2\gamma\delta(t - \tau) = \frac{\beta}{M} \langle \xi(t)\xi(\tau) \rangle. \quad (\text{A.2})$$

where M is the mass of the permeating ion, $\beta = RT$ with R the gas constant and T the absolute temperature, and $\langle \xi(t)\xi(\tau) \rangle$ indicates the temporal average.

The Langevin equation (A.1) can be solved exactly in some limiting cases or for some classes of mean field potentials, i.e., of the function $G(x)$. The solution of Eq. A.1 can be used to compute the rate of escape from metastable states, or in other words the rate constant k of escape from a well W across a barrier S . In KRT this rate constant is calculated solving Eq. A.1 within a quadratic approximation for G around x_w and x_s , i.e., the well W and the barrier S . If n_w is the equilibrium population of particles in the well and j_s is the flow of particles from W through the barrier, we have the well-known expression (Hanggi et al., 1990)

$$k = \frac{j_s}{n_w} = \frac{1}{\beta h} \left(\sqrt{\frac{\zeta^2}{4} + 1} - \frac{\zeta}{2} \right) \chi \exp(-\beta(G^{(s)} - G^{(w)})) \quad (\text{A.3})$$

where $\zeta = \gamma((1/M)G''(x_s))^{-1/2}$, $\chi = (\beta h/2\pi)((1/M)G''(x_w))^{1/2}$, $G^{(s)} = G(x_s)$, and $G^{(w)} = G(x_w)$. When the flux j from a plateau region of the free energy profile (like the interior and the exterior of a channel) has to be estimated, Eq. A.3 fails; the correct flux equation has the form $j = k\rho$, where ρ is the particle density at the plateau. Since $G''(x) = 0$ for $x < 0$ and for $x > l$ (i.e., not in the channel), a quadratic approximation for the free energy to calculate the current from these regions cannot be used. Hence, the correct limit for $G''(x_w) \rightarrow 0$ of Eq. A.3 is

$$\begin{aligned} \tilde{k} &= \frac{j_s}{\rho} = k \frac{n_w}{\rho} \\ &= k \frac{\int_{\text{well}} dx \int dv \exp\left[-\beta\left(\frac{M}{2}v^2 + G(x_w) + \frac{G''(x_w)}{2}x^2\right)\right]}{\int dv \exp\left[-\beta\left(\frac{M}{2}v^2 + G(x_w)\right)\right]} \\ &= \sqrt{\frac{1}{2\pi\beta M}} \left(\sqrt{\frac{\zeta^2}{4} + 1} - \frac{\zeta}{2} \right) \exp(-\beta(G^{(s)} - G^{(w)})) \end{aligned} \quad (\text{A.4})$$

which is independent of $G''(x_w)$.

If $\zeta \ll 1$, the effect of friction can be neglected. This takes the rate

constant of Eq. A.3 to the so-called Transition State Theory (TST) form (Hanggi et al., 1990):

$$k^{\text{TST}} = \frac{1}{\beta h} \chi \exp(-\beta(G^{(s)} - G^{(w)})) \quad (\text{A.5})$$

The condition $\zeta \ll 1$ holds as long as trajectories starting from the left side of the surface Σ (separating the two metastable states) and crossing it do not return to the left side. Since ζ (resp. χ) depends only on the local free energy profile at the barrier (resp., at the well) it is possible to define

$$\mathcal{G}^{(s)} = G^{(s)} - \frac{1}{\beta} \ln \left(\sqrt{\frac{\zeta^2}{4} + 1} - \frac{\zeta}{2} \right)$$

and

$$\mathcal{G}^{(w)} = G^{(w)} - \frac{1}{\beta} \ln \chi$$

and recast Eqs. A.3 and A.4 in the simple form

$$\begin{aligned} k &= \frac{1}{\beta h} \exp(-\beta(\mathcal{G}^{(s)} - \mathcal{G}^{(w)})) \quad \text{if } G''(x_w) > 0 \\ \tilde{k} &= \sqrt{\frac{1}{2\pi\beta M}} \exp(-\beta(\mathcal{G}^{(s)} - \mathcal{G}^{(w)})) \quad \text{if } G''(x_w) = 0 \end{aligned} \quad (\text{A.6})$$

These are the expressions for rate constants used in section on Kramer rate theory.

APPENDIX B

In this Appendix the permeability ratio P_B/P_A is computed in the strong friction and in the moderate-to-strong friction case.

Let us now consider the case in which the friction factor is large so that the inertial terms $M_A\ddot{x}_A$ and $M_B\ddot{x}_B$ can be neglected. In this case the solution of the Langevin equation can be obtained by solving the associated Fokker-Planck equation for the probability density $\rho(x, t)$ (see Risken, 1989; Melnikov, 1991; Hanggi et al., 1990) which has the form:

$$\frac{\partial \rho(x, t)}{\partial t} = \frac{1}{M\gamma} \left[\frac{\partial}{\partial x} G'(x) - \frac{FV_{\text{rev}}}{l} + RT \frac{\partial^2}{\partial x^2} \right] \rho(x, t) \quad (\text{B.1})$$

where l is the length of the channel. The stationary probability density satisfying Eq. B.1 carrying current j_A and obeying the boundary conditions for $\rho_A(0) = \rho_A$ and $\rho_A(l) = 0$ (i.e., at the right side of the channel) is

$$\begin{aligned} \rho_A(x) &= \frac{j_A}{D_A} \exp\left[-\beta\left(G_A(x) - \frac{FV_{\text{rev}}}{l}x\right)\right] \\ &\quad \int_x^l dy \exp\left[\beta\left(G_A(y) - y \frac{FV_{\text{rev}}}{l}\right)\right] \end{aligned} \quad (\text{B.2})$$

with the diffusion coefficient $D_A = RT/M_A\gamma_A$. Assuming $G_{(A,B)}(0) = 0$ (i.e., the free energy at the left and right side of the channel is set equal to zero) and $\rho_A(0) = \rho$, we have

$$\rho_A = \frac{j_A}{D_A} \int_0^l dy \exp\left[\beta\left(G_A(y) - y \frac{FV_{\text{rev}}}{l}\right)\right] \quad (\text{B.3})$$

Similarly, for ion B we have the boundary conditions $\rho_B(0) = 0$ and

$\rho_B(l) = \rho$, and consequently:

$$\rho_B = \frac{j_B}{D_B} \exp(\beta F V_{\text{rev}}) \int_0^1 dy \exp \left[\beta \left(G_B(y) - \frac{y}{l} F V_{\text{rev}} \right) \right]. \quad (\text{B.4})$$

If we impose $j_B + j_A = 0$ and $\rho_B = \rho_A$, we obtain an equation for $\exp(\beta F V_{\text{rev}})$ and defining:

$$G_{(A,B)}^{(s)} - \Delta G_{(A,B)}(x) = G_{(A,B)}(x) \quad (\text{B.5})$$

we have from Eq. 3:

$$\frac{P_B}{P_A} = \frac{D_B}{D_A} \exp(-\beta(G_B^{(s)} - G_A^{(s)})) \quad (\text{B.6})$$

$$\frac{\int_0^1 dx \exp[-\beta \Delta G_A(x)] (P_B/P_A)^{-x/l}}{\int_0^1 dx \exp[-\beta \Delta G_B(x)] (P_B/P_A)^{-x/l}}.$$

Let us now consider the moderate-to-strong friction case and assume that the permeation through the ionic channel is described as the crossing through M barriers separated by $M - 1$ wells (see Fig. 1 A). We will assume biionic conditions in which ion A is on the left side of the membrane channel, with concentration $[A]_L$, and ion B on the right, with concentration $[B]_R$. We will denote by $p_{A,i}$ (resp. $p_{B,i}$), $i = 1, \dots, M - 1$ the probability that ion A (resp. ion B) is in the well i , and by $k_{A,i}^+$ ($k_{A,i}^-$) the rate constant for a transition from well $i - 1$ to well i (resp., from i to well $i - 1$). If only one ion is present at each time in the channel, at the steady state, we have:

$$\begin{aligned} k_{1,2}^- p_{1,2} + k_{1,1}^+ [I]_L p_{\text{empty}} - (k_{1,1}^- + k_{1,2}^+) p_{1,1} &= 0 \\ k_{i,i+1}^- p_{i,i+1} + k_{i,i}^+ p_{i,i-1} - (k_{i,i}^- + k_{i,i+1}^+) p_{i,i} &= 0 \\ k_{i,M-1}^+ p_{i,M-1} + k_{i,M}^- [I]_R p_{\text{empty}} - (k_{i,M-1}^- + k_{i,M}^+) p_{i,M-1} &= 0 \end{aligned} \quad (\text{B.7})$$

where I stands for A and B and p_{empty} is the probability that the channel is not occupied, i.e., $p_{\text{empty}} = 1 - \sum_{i=1}^{M-1} (p_{A,i} + p_{B,i})$. Notice that the dimensions of $k_{i,1}^+$ and $k_{i,M}^-$ are $\text{s}^{-1} \text{mol}^{-1}$, while the dimensions of the other rate constants are s^{-1} . This difference is also evident in the microscopic determination of these rate constants: it is possible to define the probability of occupancy of a well, but the probability of occupancy of the interior (or exterior) of the channel is not well-defined (see Appendix for details). In the presence of an external potential V_{rev} , the KRT rate constants (see Appendix A) are

$$\begin{aligned} k_{i,1}^+ &= \frac{1}{\beta h} \exp(\beta(\mathcal{G}_{i,1} - \mathcal{G}_{i,1-1}^{(w)} - F l_i^+ V_{\text{rev}})) \quad i \neq 1 \\ k_{i,i}^- &= \frac{1}{\beta h} \exp(-\beta(\mathcal{G}_{i,i} - \mathcal{G}_{i,i}^{(w)} + F l_i^- V_{\text{rev}})) \quad i \neq M \\ k_{i,1}^+ &= \sqrt{\frac{1}{2\pi\beta M_1}} \exp(-\beta(\mathcal{G}_{i,1} - F l_1^+ V_{\text{rev}})) \\ k_{i,M}^- &= \sqrt{\frac{1}{2\pi\beta M_1}} \exp(-\beta(\mathcal{G}_{i,M} + F l_M^- V_{\text{rev}})) \end{aligned} \quad (\text{B.8})$$

where $\mathcal{G}_{i,i}$ is the Gibbs free energy of ion I at the barrier i , which is corrected with the factor

$$\frac{1}{\beta} \ln \left(\sqrt{\frac{\zeta_{i,i}^2}{4} + 1} - \frac{\zeta_{i,i}}{2} \right) \quad \text{with} \quad \zeta_{i,i} = \gamma_i \left(\frac{1}{M_1} G_i''(x_{s,i}) \right)^{-1/2}$$

in order to take into account diffusive corrections (see Appendix A), $\mathcal{G}_{A,i}^{(w)}$ is the Gibbs free energy in the well i , which is corrected with the factor

$$\frac{1}{\beta} \ln(\chi_i) \quad \text{with} \quad \chi_{i,i} = \frac{\beta h}{2\pi} \left(\frac{1}{M_1} G_i''(x_{w,i}) \right)$$

and l_i^+ (l_i^-) is the electric distance between well $i - 1$ and the barrier i (between well i and barrier i). For simplicity we assume the electric distances for ions with the same valence to be equal.

At the steady state, the current through the channel carried by ion I is $j_I = k_{1,M}^+ p_{1,M-1} - k_{i,1}^- p_{i,1}$. Hence, solving Eq. B.7 for the $p_{i,i}$ -s, we have

$$j_I = p_{\text{empty}} \frac{[I]_R \prod_{i=1}^M k_{i,i}^+ - [I]_L \prod_{i=1}^M k_{i,i}^-}{\sum_{i=1}^M \left(\prod_{j=1}^{i-1} k_{i,j}^- \right) \left(\prod_{h=i+1}^M k_{i,h}^+ \right)}. \quad (\text{B.9})$$

Using the zero current condition $j_A + j_B = 0$, and assuming $[A]_L = [B]_R$, $[A]_R = [B]_L = 0$, and substituting the explicit expressions for the rate constants in Eq. 16, we have the following equation for V_{rev} :

$$\exp(\beta z F V_{\text{rev}}) = \sqrt{\frac{M_A}{M_B}} \frac{\mathcal{A}}{\mathcal{B}} \quad (\text{B.10})$$

where

$$\begin{aligned} \mathcal{A} &= \sum_{i=1}^M \exp(\beta \mathcal{G}_{A,i}) \left[\prod_{j<i} \exp(-\beta F l_j - V_{\text{rev}}) \right. \\ &\quad \left. \prod_{j>i} \exp(\beta z F l_j^+ V_{\text{rev}}) \right] \\ \mathcal{B} &= \sum_{i=1}^M \exp(\beta \mathcal{G}_{B,i}) \left[\prod_{j<i} \exp(-\beta F l_j - V_{\text{rev}}) \right. \\ &\quad \left. \prod_{j>i} \exp(\beta z F l_j^+ V_{\text{rev}}) \right] \end{aligned}$$

where the relation $\sum_{i=1}^M (l_i^+ + l_i^-) = 1$ was used.

Using Eq. 3, we obtain:

$$\frac{P_B}{P_A} = \frac{\sum_{i=1}^M \exp[\beta \mathcal{G}_{A,i}] \left(\frac{P_B}{P_A} \right) \exp \left(\sum_{h=i+1}^M l_h^+ - \sum_{h=1}^{i-1} l_h^- \right)}{\sum_{i=1}^M \exp[\beta \mathcal{G}_{B,i}] \left(\frac{P_B}{P_A} \right) \exp \left(\sum_{h=i+1}^M l_h^+ - \sum_{h=1}^{i-1} l_h^- \right)} \sqrt{\frac{M_A}{M_B}} \quad (\text{B.11})$$

APPENDIX C

In this Appendix the values of hydration energies G_i used in Eq. 26 are obtained from physical quantities that can be experimentally measured, such as the total hydration energy G_{hydr} (Conway, 1981) and the Gibbs free energy G_i^{gas} of clusters composed of i water molecules and ion I^+ in the gas phase (Kearle, 1974). These data can be measured with a very good accuracy, and are reported in Table 1.

G_i^{gas} is, by definition, the Gibbs free energy of the reaction:



where $I^+(\text{H}_2\text{O})_i^{\text{gas}}$ is the cluster composed by the ion I^+ and i water molecules (the superscript *gas* stands for “from vacuum to hydrated gas phase”).

The total hydration energy G_{hydr} is the Gibbs free energy of the reaction:



where I^+_{liq} is the fully hydrated ion.

G_i is obtained by considering two different reactions: the first one corresponding to the reaction $I^+_{\text{gas}} \rightarrow I^+(\text{H}_2\text{O})_{\text{channel}}$, with Gibbs free energy $G_i^{\text{v} \rightarrow \text{c}}$ (the superscript stands for from vacuum to channel); the second corresponding to the reaction from the state I^+_{gas} to the state in which the ion is completely surrounded by the first hydration shell, with Gibbs free energy G_1 . Thus

$$G_i = G_i^{\text{v} \rightarrow \text{c}} - G_1, \quad (\text{C.1})$$

$G_i^{\text{v} \rightarrow \text{c}}$ can be estimated noticing that in the channel the i water molecules are “blocked” by the walls in a fixed position, while in the gas phase they can be in any angular position around the ion. Thus $G_i^{\text{v} \rightarrow \text{c}}$ is approximately given by

$$G_i^{\text{v} \rightarrow \text{c}} = G_i^{\text{gas}} - TS^{\text{gas}} \quad (\text{C.2})$$

where S^{gas} is the entropy due to these rotational degrees of freedom. In particular, if n_c is the primary coordination number, the independent configurations of the i molecules of water around the ions are

$$\binom{n_c}{i} = \frac{n_c(n_c - 1) \cdots (n_c - i + 1)}{i!}.$$

Hence, the entropic contribution in C.2 is given by

$$S^{\text{gas}} = R \ln \left(\frac{n_c(n_c - 1) \cdots (n_c - i + 1)}{i!} \right)$$

G_1 can be calculated from G_{hydr} subtracting the secondary shell contribution G_{II} , estimated within a Born approximation (Conway, 1981). If r_1 is the ionic radius and r_w is the effective radius of a water molecule, G_1 is given by

$$G_1 = G_{\text{hydr}} - G_{\text{II}} = G_{\text{hydr}} - \frac{z^2 e^2}{r_1 + 2r_w} \left(1 - \frac{1}{\epsilon_w} \right) \quad (\text{C.3})$$

where ϵ_w is the dielectric constant of water ($\epsilon_w \approx 78$).

Hence, using C.1, C.2 and C.3, G_i is given by

$$G_i = G_i^{\text{gas}} - G_{\text{hydr}} - RT \ln \left(\frac{n_c(n_c - 1) \cdots (n_c - i + 1)}{i!} \right) + \frac{z^2 e^2}{r_1 + 2r_w} \left(1 - \frac{1}{\epsilon_w} \right). \quad (\text{C.5})$$

This equation relates the parameters that are used in the model of ionic hydration in constrained conditions, as described in the Hydration Component section, with experimentally measurable numbers, such as n_c , r_1 , G_i^{gas} , and G_{hydr} .

Fig. 6 reproduces the values of G_i as a function of Ω for all the monovalent cations. $\Omega = 1$ corresponds to the ion with the primary hydration shell, and $\Omega = 0^+$ to the ion with two molecules of water. The consistency of the model requires the curve of every cation to go through 0 when Ω is 1, and this seems the case for every cation. Li^+ is the only ion for which we have data for hydration numbers greater than primary coordination number and, in that case, the line interpolating between G_4 and G_5 crosses the $\Omega = 1$ at $\sim 1 \text{ kcal mol}^{-1}$, and this is a value smaller or

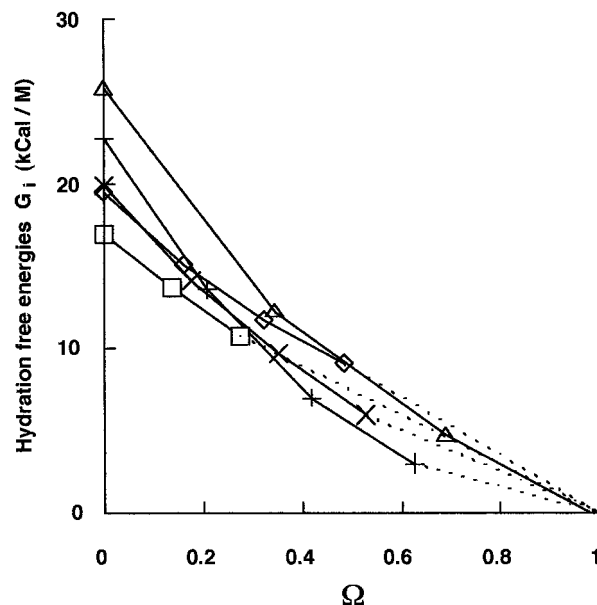


FIGURE 6 The dependence of G_i on the solid angle Ω for Li^+ (Δ), Na^+ ($+$), K^+ (\times), Rb^+ (\diamond), and Cs^+ (\square).

comparable to the experimental uncertainty in determining the G_i values. Hence, the model of hydration in constrained conditions can be considered quite satisfactory, especially in our semiquantitative theory. Table 2 reproduces all the parameters used in the model, i.e., the G_i values, the primary coordination numbers, and the Pauling ionic radii and the diffusion coefficient D .

We are grateful to Profs. O. Andersen, D. Bertrand, M. Klein, K. W. Yau and to Dr. A. Menini for comments on the manuscript, and to Drs. A. Maritan, E. Tosatti, B. Chiarotti, and G. Santoro for helpful discussions. L. Giovannelli did the artwork.

This research was supported by grants funded by the European Commission (TRANS 960593) and the Human Frontier Science Program.

REFERENCES

- Andersen, O. S. 1989. Kinetics of ion movement mediated by carriers and channels. *Methods Enzymol.* 171:62–112.
- Andersen, O. S., and R. E. Koeppe II. 1992. Molecular determinants of channel function. *Physiol. Rev.* 4:S89–S158.
- Arnold, V. I. 1985. *Dynamical Systems III*. Springer-Verlag, Berlin.
- Bek, S., and E. Jacobsson. 1994. Brownian dynamics study of a multiply occupied cation channel. *Biophys. J.* 66:1029–1038.
- Blades, A. T., P. Jayaweem, M. G. Ikononon, and P. Kebarle. 1990. Studies of alkaline earth and transition metal M^{++} gas phase ion chemistry. *J. Chem. Phys.* 10:5900–5906.
- Brooks III, C., M. Karplus, and B. M. Pettit. 1988. *Proteins: A Theoretical Perspective of Dynamics, Structure and Thermodynamics*. John Wiley & Sons, New York.
- Chiamvimonvat, N., M. T. Perez-Garcia, G. T. Tomaselli, and E. Marban. 1996. Control of ion flux and selectivity by negatively charged residues in the outer mouth of the rat sodium channels. *J. Physiol. (Lond.)* 491:51–59.
- Conway, B. E. 1981. *Ionic Hydration in Chemistry and Biophysics*. Elsevier Science, New York.
- Cooper, K. E., P. Y. Gates, and R. S. Eisenberg. 1988a. Diffusion theory and discrete rate constants in ion permeation. *J. Membr. Biol.* 106:95–105.

- Cooper, K. E., P. Y. Gates, and R. S. Eisenberg. 1988b. Surmounting barriers in ionic channels. *Q. Rev. Biophys.* 21:331–364.
- Cooper, K. E., E. Jakobsson, and P. G. Wolynes. 1985. The theory of ion transport through membrane channels. *Prog. Biophys. Mol. Biol.* 46: 51–96.
- Creighton, T. E. 1993. *Proteins*. W. H. Freeman and Co., New York.
- Dorman, D., M. B. Partenskii, and P. C. Jordan. 1996. A semi-microscopic Monte Carlo study of permeation energetics in a gramicidin-like channel. *Biophys. J.* 70:121–134.
- Doyle, D. A., J. M. Cabral, R. A. Pfuetzner, A. Kuo, J. M. Gulbis, S. L. Cohen, B. T. Chait, and R. MacKinnon. 1998. The structure of the potassium channel: molecular basis of K^+ conduction and selectivity. *Science*. 280:69–77.
- Dwyer, T. M., D. J. Adams, and B. Hille. 1980. The permeability of the endplate channel to organic cations in frog muscle. *J. Gen. Physiol.* 75:469–492.
- Eisenman, G. 1962. Cation selective electrodes and their mode of operation. *Biophys. J. (Suppl.)*. 2:259–323.
- Eisenman, G. 1963. The influence of Na, K, Li, Rb and Cs on cellular potentials and related phenomena. *Bol. Inst. Estud. Med. Biol.* 21: 155–183.
- Eisenman, G., and R. Horn. 1983. Ionic selectivity revisited: The role of kinetic and equilibrium processes in ionic permeation through channels. *J. Membr. Biol.* 76:197–225.
- Eisenman, G., and S. Krasne. 1975. The ionic selectivity of carrier molecules, membranes and enzymes. In *MTP International Review of Science*, Vol. 2. Butterworths, London. 27–59.
- Eismann, E., F. Muller, S. Heinemann, and B. Kaupp. 1994. A single negative charge within the pore region of a cGMP-gated channel controls rectification. *Proc. Natl. Acad. Sci. USA*. 91:1109–1113.
- Eyring, H., R. Lumry, and J. W. Woodbury. 1949. Some applications of modern rate theory to physiological systems. *Record Chem. Prog.* 10: 100–114.
- Faure, I., E. Moczydlowski, and L. Schild. 1996. On the structural basis for ionic selectivity among Na^+ , K^+ , and Ca^{2+} in the voltage-gated sodium channel. *Biophys. J.* 71:3110–3125.
- Fuller, C. M., B. K. Berdiev, V. G. Shlyonsky, I. I. Ismailov, and D. J. Benos. 1997. Point mutations in abENaC regulate channel gating, ion selectivity, and sensitivity to amiloride. *Biophys. J.* 72:1622–1632.
- Galzi, J., L. A. Devillers-Theiry, N. Hussy, S. Bertand, J. P. Changeux, and D. Bertand. 1992. Mutations in the channel domain of a neuronal nicotinic receptor convert ion selectivity from cationic to anionic. *Nature*. 359:500–505.
- Gardiner, C. W. 1985. *Handbook of Stochastic Methods*. Springer-Verlag, Berlin.
- Glendening, E. D., and D. Feller. 1995. Cation-water interactions: the $M^+(H_2O)_n$ cluster for alkali metals, $M = Li, Na, K, Rb$ and Cs . *J. Phys. Chem.* 99:3060–3067.
- Hagiwara, S., and K. Takahashi. 1974. The anomalous rectification and cation selectivity of the membrane of a starfish egg cell. *J. Membr. Biol.* 18:61–80.
- Hanggi, P., P. Talkner, and M. Borkovec. 1990. Reaction-rate theory: fifty years after Kramer. *Rev. Mod. Phys.* 62:251–339.
- Heginbotham, L., Z. Lu, T. Abramson, and R. MacKinnon. 1994. Mutations in the K^+ channel signature sequence. *Biophys. J.* 66:1061–1067.
- Heinemann, S. H., H. Terlau, W. Stuehmer, K. Imoto, and S. Numa. 1992. Calcium channel characteristics conferred on the sodium channel by single mutations. *Nature*. 356:441–443.
- Hille, B. 1975a. Ionic selectivity of Na and K channels of nerve membranes. In *Membranes: A Series of Advances*, Vol. 3. G. Eisenman, editor. Marcel Dekker, New York.
- Hille, B. 1975b. Ionic selectivity saturation and block in sodium channels. A four barrier model. *J. Gen. Physiol.* 66:535–550.
- Hille, B. 1992. *Ionic Channels of Excitable Membranes*. Sinauer Associates, Sunderland, MA.
- Imoto, K., C. Busch, B. Sackmann, M. Mishina, T. Konno, J. Nakai, H. Bujo, and S. Numa. 1988. Rings of negatively charged amino acids determine the acetylcholine receptor channel conductance. *Nature*. 335: 645–651.
- Kearle, P. 1974. *Modern Aspects of Electrochemistry*, Chap. 1, Vol. 11. B. E. Conway and J. O. M. Bockris, editors. Plenum Publishing, New York.
- Kim, M.-K., T. Morii, L.-X. Sun, K. Imoto, and Y. Mori. 1993. Structural determinants of ion selectivity in brain calcium channel. *FEBS Lett.* 318:145–148.
- Kirsch, G. E., J. M. Pascual, and C. C. Shieh. 1995. Functional role of a conserved aspartate in the external mouth of voltage-gated potassium channels. *Biophys. J.* 68:1804–1813.
- Krasne, S., and G. Eisenman. 1973. The molecular basis of ion selectivity. In *Membranes: A Series of Advances*, Vol. 2. G. Eisenman, editor. Marcel Dekker, New York.
- Kumpf, R. A., and D. A. Dougherty. 1993. A mechanism for ion selectivity in potassium channels: computational studies of cation- π interactions. *Science*. 261:1708–1710.
- Lauger, P. 1973. Ion transport through pores: a rate theory analysis. *Biochim. Biophys. Acta*. 311:423–441.
- Levitt, D. G. 1991. General continuum theory for multiion channel. *Biophys. J.* 59:271–277.
- Lipkind, G. M., and H. A. Fozzard. 1995. A structural motif for the voltage gated potassium channel pore. *Proc. Natl. Acad. Sci. USA*. 92: 9215–9219.
- Melnikov, V. I. 1991. The Kramers problem: fifty years of development. *Phys. Rep.* 209:1 and 2:1–71.
- Menini, A. 1990. Currents carried by monovalent cations through cyclic GMP-activated channels in excised patches from salamander rods. *J. Physiol.* 424:167–185.
- Myers, V. B., and D. A. Haydon. 1972. Ion transfer across lipid membranes in the presence of gramicidin A. II. The ion selectivity. *Biochim. Biophys. Acta*. 274:313–322.
- Perez-Cornejo, P., and T. Begenish. 1994. The multi-ion nature of the pore in *Shaker K⁺* channels. *Biophys. J.* 66:1929–1938.
- Picco, C., and A. Menini. 1993. The permeability of the cGMP-activated channel to organic cations in retinal rods of the tiger salamander. *J. Physiol.* 460:741–758.
- Reuter, H., and C. Stevens. 1980. Ion conductance and ion selectivity of potassium channels in snail neurons. *J. Membr. Biol.* 57:103–118.
- Risken, H. 1989. *The Fokker-Planck Equation*. Springer-Verlag, Berlin.
- Roux, B. 1996. Valence selectivity of the gramicidin channel: a molecular dynamics free energy perturbation study. *Biophys. J.* 71:3177–3185.
- Roux, B., and M. Karplus. 1991. Ion transport in a model gramicidin channel. *Biophys. J.* 59:961–981.
- Roux, B., and M. Karplus. 1993. Ion transport in the gramicidin channel: free energy of the solvated right-handed dimer in a model membrane. *J. Am. Chem. Soc.* 115:3250–3262.
- Roux, B., and M. Karplus. 1994. Molecular dynamics simulations of the gramicidin channel. *Annu. Rev. Biomol. Struct. Dyn.* 23:731–761.
- Segonella, D. E., H. Laasonen, and M. L. Klein. 1996. Ab initio molecular dynamics study of proton transfer in a polyglycine analog of the ion channel gramicidin A. *Biophys. J.* 71:1172–1178.
- Sesti, F., M. Nizzari, and V. Torre. 1996. Effect of changing temperature on the ionic permeation through the cyclic GMP-gated channel from vertebrate photoreceptors. *Biophys. J.* 70:2616–2639.

- Slesinger, P. A., Y. N. Yan, and L. Y. Yan. 1993. The S4-S5 loop contributes to the ion selective pore of potassium channels. *Neuron*. 11:739-749.
- Starkus, J. G., L. Kuschel, M. D. Rayner, and S. H. Heinemann. 1997. Ion conduction through C-type inactivated *Shaker* channels. *J. Gen. Physiol.* 110:539-550.
- Wallace, B. A. 1990. Gramicidin channels and pores. *Annu. Rev. Biophys. Chem.* 19:127-157.
- Woodbury, J. W. 1971. Eyring-rate theory model of the current-voltage relationships of ion channels in excitable membranes. In *Chemical Dynamics: Papers in Honor of Henry Eyring*. J. O. Hirschfelder, editor. Wiley, New York.
- Wu, J. 1991. Microscopic model for selective permeation in ion channels. *Biophys. J.* 60:238-251.
- Yang, J., P. T. Ellinor, W. A. Sather, J-F. Zhang, and R. W. Tsien. 1993. Molecular determinants of Ca selectivity and ion permeation in L-type Ca channels. *Nature*. 366:158-161.
- Yool, A. J., and T. L. Schwartz. 1991. Alteration of ionic selectivity of a K^+ channel by mutation of the H5 region. *Nature*. 349:700-704.